

## **Main revisions and response to reviewers' comments**

Manuscript No.: acp-2019-689

Title: Quantification and evaluation of atmospheric ammonia emissions with different methods: A case study for the Yangtze River Delta region, China

Authors: Yu Zhao, Mengchen Yuan, Xin Huang, Feng Chen, Jie Zhang

We thank very much for the valuable comments and suggestions from the two reviewers, which help us improve our manuscript significantly. The comments were carefully considered and revisions have been made in response to suggestions. Following is our point-by-point responses to the comments and corresponding revisions.

### **Reviewer #2**

*0. This paper compares and contrasts two methodologies for estimating emissions of NH<sub>3</sub> in China, and illustrates the consequence through model simulations. The paper deals with an important subject, since the large uncertainties surrounding ammonia emissions need to be understood by modelers and policy experts. The paper is generally well written, and generally sound.*

### **Response and revisions:**

We appreciate the reviewer's positive remarks on the importance of the work.

*1. I miss consideration of many of the factors omitted from the emission estimation procedure. This study basically used temperature, and agricultural statistics, to calculate emission factors (EFs). However, with respect to emissions from livestock/poultry, wind-speed is also a very important factor (e.g. Gyldenkaerne et al.,*

2005, Skjoeth et al., 2011, Flechard et al., 2013). Many other factors should also impact  $\text{NH}_3$  emissions, such as radiation, rainfall (and other precipitation), leaf-wetness, atmospheric stability, large uncertainties in the so-called Gamma factors, or bi-directional exchange in general (Bash et al., 2013, Flechard et al., 2013, Massad et al., 2010, Wichink Kruit et al., 2012). Consideration of such factors might also help to explain some of the model discrepancies outlined in Section 3, and should at least be considered before trying to explain all such discrepancies in terms of temperature and a few selected variables only

### **Response and revisions:**

We thank and agree the reviewer's important comment. In this work, we mainly compared the magnitude and the spatial and temporal distribution of the YRD  $\text{NH}_3$  emissions estimated with two different methodologies, and evaluated the two inventories through air quality modeling based on available satellite and ground observation within the region. Compared to E1, in particular, E2 included the impacts of the growing and farming cycles, soil properties (pH) and selected meteorological factor (temperature) on  $\text{NH}_3$  emissions for fertilizer using sector, and those of manure management processes and ambient temperature for livestock/poultry breeding. Besides the parameters we are concerned with, however, some other factors and processes also play important roles on atmosphere-land exchange of  $\text{NH}_3$ , as pointed by the reviewer. Those factors/processes that were not considered in this work include given meteorological factors (e.g., wind speed, precipitation and leaf surface wetness), surface layer turbulence, air and surface heterogeneous-phase chemistry, and plant physiological conditions (Flechard et al., 2013). In general, those factors/processes could be integrated in the bi-directional surface-atmosphere exchange module coupled in the air quality modeling, and improved estimation of  $\text{NH}_3$  flux (emissions and depositions) were expected. The modeling system with the bi-directional  $\text{NH}_3$  exchange were reported to be able to reduce the biases and error in simulation of  $\text{NH}_x$  ( $\text{NH}_3 + \text{NH}_4^+$ ) wet deposition and ambient aerosol concentrations for both US and Europe (Bash et al., 2013; Wichink Kruit et al., 2012). Limited studies on the

bi-directional NH<sub>3</sub> exchange were found for China (e.g., Fu et al., 2015). Out of the scope of current work, we did not focus on the bi-directional NH<sub>3</sub> exchange module and did not include the module for emission evaluation and comparison. We agree with the reviewer that the ignorance of given parameters/process in the estimation could potentially further explain the discrepancy between the simulation and observation. A more comprehensive evaluation and comparison in NH<sub>3</sub> emission inventories was thus suggested in the future, including the bi-directional NH<sub>3</sub> exchange and the top-down constraint with inversed modeling.

We have discussed this limitation and added relevant literatures **in lines 561-580, page 18 in the revised manuscript.**

*2. The authors use meteorology from ECMWF for their emissions, but why not the WRF model, since that is obviously available and is used for their CMAQ runs?*

**Response and revisions:**

We thank the reviewer's comment. We do not have very specific reason for using the ECMWF instead of WRF. When calculating the emissions, the underlying data open to the public were preferentially selected. ECMWF provided daily average data that satisfied our need of emission estimation and they were open to the public, thus we selected the dataset.

*3. The equations used are generally clearly written out, although it isn't always clear where they are coming from. For example, is it correct that equations 2 & 3 are a mixture of methods from Huang et al 2012 and EEA 2013? On the other hand, I read in various sections of EEA 2013 that temperature functions could not be provided (e.g. chap. 3.D crop production and agricultural soils) If from EEA, then it would also be good to cite the scientific papers underlying the EEA guidelines, and to be more specific as to which sections of EEA are being cited (it is a monster document).*

**Response and revisions:**

We appreciate the reviewer's comment. The specific EEA guidelines (EEA 2013a; 2013b; 2009) were provided in the revised manuscript. For Eq. 2 & 3, in particular, the linear relationships between NH<sub>3</sub> volatilization rate and temperature/soil pH were described in Chap. 4.D crop production and agricultural soils of EEA (2009)/Huang et al. (2012), and we specified them respectively **in lines 227-228, page 8 and lines 211-212, page 7 in the revised manuscript.**

**4. Some other points:**

*P2. The abstract is rather long, and should be shortened for clarity.*

**Response and revisions:**

We thank the reviewer's comment and the abstract was shortened.

*P3, L67. NH<sub>3</sub> is said to react with NO<sub>x</sub>, but NO<sub>x</sub> usually means NO+NO<sub>2</sub>. I think the authors mean HNO<sub>3</sub>?*

**Response and revisions:**

We thank the reviewer's reminder and it is corrected as nitric acid (HNO<sub>3</sub>) in the revised manuscript.

*P3, L78-81. The sentence is a little unclear. Clarify.*

**Response and revisions:**

We thank the reviewer's comment. We mean that SO<sub>2</sub> and NO<sub>x</sub> emissions have gradually decreased due to improved control, thus the NH<sub>3</sub> emissions was found to play a greater role on the secondary aerosol formation and nitrogen deposition, compared to previous years. The sentence is rewritten **in lines 72-76, page 3 in the**

**revised manuscript:**

Recently the SO<sub>2</sub> and NO<sub>x</sub> emissions have gradually decreased due to implementation of various pollution control measures in China, thus NH<sub>3</sub> emissions were found to play a greater role on secondary aerosol formation and nitrogen deposition compared to previous years.

*P4, L112. Methods of including meteorology in NH<sub>3</sub> emissions have been around for some time and should be mentioned, e.g. Gyldenkaerne et al., 2005, Skjoeth et al., 2011, Wichink Kruit et al., 2012, Bash et al., 2013.*

**Response and revisions:**

We thank and agree the reviewer's comment. We have added the relevant papers and description **in lines 110-111, page 4 in the revised manuscript.**

*P5, L148. Another source of human-related NH<sub>3</sub> emissions is pets. As shown in e.g. Sutton et al 1995, 2000, human pets can be as significant as human metabolism with regard to NH<sub>3</sub> emissions.*

**Response and revisions:**

We thank and agree the reviewer's comment. Due to lack of detailed statistic, we did not include pet emissions in current NH<sub>3</sub> inventories. Given the relatively small fraction in total emissions (e.g., less than 2% for United Kingdom by Sutton et al.), we believe that the uncertainty was limited. We have added the explanation **in lines 149-152, page 5 in the revised manuscript.**

*P6, L168. Using should be used.*

**Response and revisions:**

We thank the reviewer's reminder and it is corrected in the revised manuscript.

*P7, L187. Give reference for radiometer*

**Response and revisions:**

We thank the reviewer's reminder and the reference for radiometer is given in the revised manuscript (Davies et al., 2009).

*P7, L202. The study of Huang et al 2012 uses a linear relationship between pH and EF. Why is the relation here said to be near-linear?*

**Response and revisions:**

We thank the reviewer's reminder and it is corrected as linear in the revised manuscript.

*P7. What is the time-resolution of the EF calculations?*

**Response and revisions:**

The time-resolution of EF calculation is monthly. In the method, the fertilization method (top or basal dressing) was month-dependent, and monthly average temperature was applied for the EF calculation. We have added the information **in lines 212-213, page 7 and line 220, page 8 in the revised manuscript.**

*P8, L232. Surely fertilizer application at 15-20cm affects the pH of the soil; doesn't this affect the assumptions made when using global pH data from IIASA?*

**Response and revisions:**

We thank and agree the reviewer's comment. Previous domestic experimental studies

in China (e.g, Zhong et al., 2006) indicated that the fertilizer application would increase the soil pH, particularly for the acidic soils. Bias thus existed in soil pH from the global database, without considering the detailed schedule and method of fertilizer application. As the quantitative relation between the fertilizer application and soil pH was still lacking at the regional scale in China, we ignored the interaction between the fertilizer application and soil pH in Eqs.(2). We acknowledged the limitation and added the explanation **in lines 243-248, page 8 in the revised manuscript.**

*P9. The basic references of the CMAQ model should be given, not just a web-address.*

**Response and revisions:**

We thank the reviewer's reminder and the basic operational guidance of CMAQ by University of North Carolina was provided in the revised manuscript (UNC, 2010).

*P10. Which version of MEGAN was used? Did you use data provided by Sindelarova, or did you use the MEGAN model itself? If the latter, a Guenther et al ref would seem more*

**Response and revisions:**

We thank the reviewer's comment. We used the MEGAN 2.1. The literature (Guenther et al., 2012) has been added in the revised manuscript.

*P10. Again, give reference to the model developers - this time for WRF.*

**Response and revisions:**

*We thank the reviewer's reminder* and the reference of WRF is provided in the revised manuscript (Skamarock et al., 2008).

*P11. The Lanciki 2018 reference for MARGA is missing.*

**Response and revisions:**

We thank the reviewer's reminder and the information of Lanciki (2018) is provided in the revised manuscript.

*P15. The citation of Wei et al (2015) is in Chinese, and thus not helpful for most authors. This instrument has been around for many years, and the artifacts documented elsewhere. Please find some citations in English for the problems mentioned.*

**Response and revisions:**

We thank the reviewer's comment and provided English papers for the problem **in lines 484-485, page 16 in the revised manuscript.** (Chen et al., 2017; Schaap et al., 2011; Stieger et al., 2018).

*P28, Use molecule not "mole.", to avoid confusion with the mole unit.*

**Response and revisions:**

We thank the reviewer's reminder and molecule is used in the revised manuscript.

*P31. Table 3. Correlation coefficients should be added, and the time-resolution of the statistics mentioned.*

**Response and revisions:**

We thank the reviewer's comment. The correlation coefficients between the observation and simulation were added in the revised Table 3, and the time-resolution of the statics was hourly, as mentioned in the revised caption of the table.



*P31 cont. for all Tables make it clear if statistics are calculated from hourly, daily or monthly values.*

**Response and revisions:**

We thank the reviewer's reminder. The statistics in Tables 3 and 6 were calculated based on the hourly values, and those in Tables 4 and 5 were from the daily values (the value of one hour (9:30am for satellite observation and the average of 9:00am-10:00am for simulation) per day). The information has been added **in the revised captions of Tables 3-6.**

*There are small English misses throughout, for example with regard to singular or plural, or omission of the definite article (the).*

**Response and revisions:**

We thank the reviewer's comment and the grammar errors are corrected in the revised manuscript.

**References**

Bash, J. O., Cooter, E. J., Dennis, R. L., Walker, J. T., Pleim, J. E.: Evaluation of a regional air-quality model with bidirectional NH<sub>3</sub> exchange coupled to an agroecosystem model, *Biogeosciences*, 10, 1635-1645, 2013.

Chen, X., Walker, J. T., Geron, C.: Chromatography related performance of the Monitor for Aerosols and Gases in ambient air (MARGA): laboratory and field-based evaluation, *Atmos. Meas. Tech*, 10, 3893-3908, 2017.

Davies, D. K., Ilavajhala, S., Wong, M. M., and Justice, C. O.: Fire Information for Resource Management System: Archiving and Distributing MODIS Active Fire Data, *IEEE Geosci. Remote Sens.*, 47, 72-79, 2009.

European Environment Agency (EEA): EMEP/CORINAIR Air Pollutant Emission Inventory Guidebook-2013, 3.B Manure management, available at: <https://www.eea.europa.eu/publications/emep-eea-guidebook-2013/part-b-sectoral-guidance-chapters/4-agriculture/3-b-manure-management/view> (last access: 25 Feb 2020), 2013a.

European Environment Agency (EEA): EMEP/CORINAIR Air Pollutant Emission Inventory Guidebook-2013, 3.D Crop production and agricultural soils, available at: <https://www.eea.europa.eu/publications/emep-eea-guidebook-2013/part-b-sectoral-guidance-chapters/4-agriculture/3-d-crop-production/view> (last access: 25 Feb 2020), 2013b.

European Environment Agency (EEA): EMEP/CORINAIR Air Pollutant Emission Inventory Guidebook-2009, 4.D Crop production and agricultural soils, available at: <https://www.eea.europa.eu/publications/emep-eea-emission-inventory-guidebook-2009/part-b-sectoral-guidance-chapters/4-agriculture/4-d/4-d-crop-production-and-agricultural-soils.pdf/view> (last access: 25 Feb 2020), 2009.

Flechard, C. R., Massad, R.-S., Loubet, B., Personne, E., Simpson, D., Bash, J. O., Cooter, E. J., Nemitz, E., Sutton, M. A.: Advances in understanding, models and parameterizations of biosphere-atmosphere ammonia exchange, *Biogeosciences*, 10, 5183-5225, 2013.

Fu, X., Wang, S., Ran, L., Pleim, J. E., Cooter, E., Bash, J. O., Benson, V., Hao, J.: Estimating NH<sub>3</sub> emissions from agricultural fertilizer application in China using the bi-directional CMAQ model coupled to an agro-ecosystem model. *Atmos. Chem. Phys.*, 15, 6637-6649, 2015

Guenther, A. B., Jiang, X., Heald, C. L., Sakulyanontvittaya, T., Duhl, T., Emmons, L. K., Wang, X.: The Model of Emissions of Gases and Aerosols from Nature version 2.1 (MEGAN2.1): an extended and updated framework for modeling biogenic emissions. *Geosci. Model Dev.*, 5, 1471-1492, 2012.

Lanciki, A.: 2060 MARGA Monitor for AeRosols and Gases in ambient Air. Metrohm Process Analytics, Switzerland, available at: <https://www.metrohm.com/en/products/process-analyzers/applikon-marga/> (last access: 10 Feb 2020), 2018.

Schaap, M., Otjes, R. P., Weijers, E. P.: Illustrating the benefit of using hourly monitoring data on secondary inorganic aerosol and its precursors for model evaluation. *Atmos. Chem. Phys.*, 11, 11041–11053, 2011

Skamarock, W. C., Klemp, J. B., Dudhia, J., Gill, D. O., Barker, D. M., Duda, M. G., Huang, X.-Y., Wang, W., Powers, J. G. A Description of the Advanced Research WRF Version 3. NCAR Tech. Note NCAR/TN-475+STR, 113 pp.doi:10.5065/D68S4MVH, 2008.

Stieger, B., Spindler, G., Fahlbusch, B. Muller, K., Gruner, A., Poulain, L., Thoni, L., Seitler, E., Wallasch, M., Herrmann, H.: Measurements of PM<sub>10</sub> ions and trace gases with the online system MARGA at the research station Melpitz in Germany - A five-year study. *J. Atmos. Chem.*, 75, 33-70, 2018.

University of North Carolina at Chapel Hill (UNC): Operational Guidance for the Community Multiscale Air Quality (CMAQ) Modeling System Version 4.7.1 (June

2010 Release), available at <http://www.cmaq-model.org> (last access: 10 Feb 2020), 2010.

Wichink Kruit, R. J., Schaap, M., Sauter, F. J., van Zanten, M. C., van Pul, W. A. J.: Modeling the distribution of ammonia across Europe including bi-directional surface atmosphere exchange, *Biogeosciences*, 9, 5261-5277, 2012.

Zhong, N., Zeng, Q., Zhang, L., Liao, B., Zhou, X., Jiang, J.: Effects of acidity and alkalinity on urea transformation in soil, *Chinese Journal of Soil Science*, 37, 1123-1128, 2006 (in Chinese).

### **Reviewer #3**

*0. The manuscript develops and presents two gridded NH<sub>3</sub> emission inventories, one based on emission factors from the literature and a second with more process information. The two are compared against one other, as well as to two ground sites. CMAQ output was also be compared against satellite columns. This is a good exploration of what is known about NH<sub>3</sub> emission patterns in the heavily populated Yangtze River Delta region. That said, without well understanding the methods E1 and E2, it was difficult to fully review manuscript.*

#### **Response and revisions:**

We appreciate the reviewer's positive remarks on the importance of the work.

*1. Emission inventories with general emission factors or more detailed process have always been used, so at first read I am not sure why this is considered as case study of the methodology versus something like "Quantification and evaluation of atmospheric ammonia emissions for the Yangtze River Delta region, China". The exact methods used for E1 and E2 are fairly confusing. The "constant emission factors" method that is referenced throughout are actually based on annual emission factors, with a monthly and spatial allocation schemes given on L179-L188. This needs to be clearer early on in the manuscript. Also, to confirm, neither allocation affects the total yearly emission? Are the activity factors different in E1 than what are used in E2?*

#### **Response and revisions:**

We appreciate the reviewer's important comment and acknowledged that some descriptions on the principles of the two methods were unclear in the original manuscript. The reviewer was correct for E1. It was developed based on the constant annual emission factors at the prefectural city level (as most of the activity data could be obtained at the prefectural city level). Spatial and monthly allocations of emissions

were then conducted, without changes in total yearly emissions. Following the reviewer's suggestion, we mentioned this at the beginning of Section 2.1 (**lines 143-145, page 5 in the revised manuscript**). It is a relatively quick and simple method, based on the previous understanding of NH<sub>3</sub> emissions at regional scale (both the emission factor and temporal distribution). The effects of actual environmental conditions and agricultural activities on emission rate were not considered at a high temporal and spatial resolution.

In E2, the method for fertilizer application and livestock/poultry breeding (the main source categories of NH<sub>3</sub>) was improved. In particular, the emission factors were developed at the monthly resolution, integrating the effects of soil, meteorology and agricultural processes. Therefore the method did not only change the temporal pattern of emissions but also the magnitude of the annual emissions, as the emission factors developed in this method varied from the ones applied in E1, which were directly taken from previous studies.

It should also be noted that the annual activity data were the same for the two inventories at the prefectural city level, although the monthly distributions were different. We have clearly stated the relation between the activity data in the two inventories **in lines 196-197, page 7 in the revised manuscript**. Please also see our response to Question 2 of the reviewer.

*2. Sect 2.2.1 about E2: please check each use of 'corrected' to make sure it is clear what/how/why something is being corrected. Specifically, L198 why does the fertilizer use need to be corrected? Where do the relationships in Table S2 come from?*

**Response and revisions:**

We appreciate the reviewer's comment and acknowledged some "corrected" were confusing. In E2, the emissions from fertilizer use and livestock/poultry breeding were recalculated with a different method from E1. In general, it is not a correction of E1. Therefore we deleted unnecessary "corrected" in the methodology section of E2

(Section 2.2). Regarding the word “corrected” fertilizer as pointed by the reviewer, in particular, we actually means that the monthly fertilizer used was estimated in E2 combining the information of investigated farming cycles. The annual total fertilizer was the same as E1. We also added an example of early-season rice for better understanding the method. The relevant texts have been revised **in lines 199-209, page 7 in the revised manuscript.**

Regarding Table S2, we clearly stated that the annual total amount of fertilizer used were the same by prefecture city and type in the two inventories **in lines 196-197, page 7 in the revised manuscript.** The method of estimating the annual amount of fertilizer by prefecture city and type in Table S2 was described in lines **in lines 165-171, page 6 in the revised manuscript.**

*3. Specific technical/style: L206 EFbase -> EFbasal and Tbase -> Tbasal*

**Response and revisions:**

We thank the reviewer’s reminder and terms are corrected in the revised manuscript.

*L206-207 Are Tbasal and T0 in different units? Otherwise, 273.15 wouldn’t be needed*

**Response and revisions:**

We thank the reviewer’s reminder and 273.15 was deleted in the revised manuscript.

*L213 ‘method’ -> ‘application method’? (if I’m guessing correctly). What are the possible methods?*

**Response and revisions:**

We thank the reviewer’s reminder and it is revised as application method (basal dressing).

*L347-L349 where is this shown about the EFs being from hot seasons?*

**Response and revisions:**

We appreciate the reviewer's comment. Most of the measurements on emission factor of ammonia from fertilizer application were conducted in summer or late spring (Cai et al., 2002; Huo et al., 2015; Su et al., 2006), especially those using micrometeorological method. It is expectable since that the basal dressing of single-season rice and maize as well as top dressing of wheat are usually conducted in late spring or summer. However, the crop rotation varies a lot in China, and part of the nitrogen-containing fertilizer actually is not applied in hot seasons. Emission estimation based on those emission factors may thus overestimate the emission intensity of ammonia (Huo et al., 2015; Wang et al., 2011; Zhang et al., 2010). We have provided relevant literatures and added the above discussion **in lines 361-369, page 12 in the revised manuscript.**

*L518-L519 Please reword. IASI is an instrument, so it cannot 'provide' an averaging kernel.*

**Response and revisions:**

We thank the reviewer's reminder and the sentence is rewritten **in lines 537-538, page 17 in the revised manuscript:**

As the ESPRI product of NH<sub>3</sub> VCDs we applied in the study does not provide the averaging kernel...

*Figure 1 caption: "Studying area and research domain" -> aren't study area and research domain the same?*

**Response and revisions:**

We thank the reviewer's reminder, and they are the same. We delete the "Studying area" in the figure caption.

*Figure 3 and Figure 6: ‘Januray’ -> “January”*

**Response and revisions:**

We thank the reviewer’s reminder and the errors are corrected.

*Figure 4: emissions misspelled in the y-axis label Figure 4: Suggest giving fertilizer and livestock consistent colors, then keeping E1 as solid fill but E2 as hatched for easier reading*

**Response and revisions:**

We thank the reviewer’s reminder and the figure is improved as required.

*Figure 6: colorscales could have greater consistency*

**Response and revisions:**

We thank the reviewer’s reminder and the figure is improved as required.

*Figure 9: the subplots should have a consistent axis font size*

**Response and revisions:**

We thank the reviewer’s reminder and the same font size is applied in all the subplots.

*Figure 10; from caption, shouldn’t axis limits be same as Figure 9? Also, helpful to add the border lines like in Figure 9 so one is orientated where they are looking*

**Response and revisions:**

We thank the reviewer’s reminder and revised the axis limits. The border lines have also been added in the revised Figure 10.



*Figure S4: there is one main cluster of data along the black line, but why is there seem to also be a second one? Also, what is the significance of the red dots, which do not fit well especially for the ABC panel?*

### **Response and revisions:**

The black line is obtained through linear regression based on all the blue dots (including the “second cluster” mentioned by the reviewer).

Different from blue dots that are calculated for all the grids within the research domain of this study, the red dots are taken from available field measurement studies, as we mentioned in the figure caption. The gap between them, in particular at lower soil pH, explained the possible uncertainty in current method, i.e., the current linear assumption between the soil pH and NH<sub>3</sub> volatilization rate might not be appropriate for soil with low pH values for eastern China. We discuss it **in lines 553-560, page 18 in the revised manuscript.**

### **References**

- Cai, G. X., Chen, D. L., Ding, H., Pacholski, A., Fan, X. H., Zhu, Z. L.: Nitrogen losses from fertilizers applied to maize, wheat and rice in the North China Plain. *Nutr. Cycl. Agroecosys.*, 63, 187-195, 2002.
- Huo, Q., Cai, X., Kang, L., Zhang, H., Song, Y., Zhu, T.: Estimating ammonia emissions from a winter wheat cropland in North China Plain with field experiments and inverse dispersion modeling, *Atmos. Environ.*, 104, 1-10, 2015.
- Su, F., Huang, B., Ding, X., Gao, Z., Chen, X., Zhang, F., Kogge, M., Römheld, V.: Ammonia volatilization of different nitrogen fertilizer types, *Soils*, 38, 682-686, 2006 (in Chinese).
- Wang, S., Xing, J., Jang, C., Zhu, Y., Fu, J. S., Hao, J.: Impact assessment of ammonia emissions on inorganic aerosols in East China using response surface modeling technique. *Environ. Sci. Technol.*, 45, 9293-9300, 2011.
- Zhang, Y., Dore, A. J., Ma, L., Liu, X., Ma, W., Cape, J. N., Zhang, F.: Agricultural ammonia emissions inventory and spatial distribution in the North China Plain. *Environ. Pollut.*, 158, 490-501, 2010.

1  
2 **Quantification and evaluation of atmospheric ammonia**  
3 **emissions with different methods: A case study for the**  
4 **Yangtze River Delta region, China**  
5

6 Yu Zhao<sup>1,2\*</sup>, Mengchen Yuan<sup>1</sup>, Xin Huang<sup>3</sup>, Feng Chen<sup>4</sup>, Jie Zhang<sup>4</sup>  
7

8 1. State Key Laboratory of Pollution Control & Resource Reuse and School of the  
9 Environment, Nanjing University, 163 Xianlin Ave., Nanjing, Jiangsu 210023, China

10 2. Jiangsu Collaborative Innovation Center of Atmospheric Environment and  
11 Equipment Technology (CICAEET), Nanjing University of Information Science &  
12 Technology, Jiangsu 210044, China

13 3. School of Atmospheric Science, Nanjing University, 163 Xianlin Ave., Nanjing,  
14 Jiangsu 210023, China

15 4. Jiangsu Provincial Academy of Environmental Science, 176 North Jiangdong Rd.,  
16 Nanjing, Jiangsu 210036, China

17  
18 \*Corresponding author: Yu Zhao

19 Phone: 86-25-89680650; email: [yuzhao@nju.edu.cn](mailto:yuzhao@nju.edu.cn)  
20

## Abstract

To explore the effects of data and method on emission estimation, two inventories of NH<sub>3</sub> emissions of the Yangtze River Delta (YRD) region in eastern China were developed for 2014 based on the constant emission factors (E1) and those characterizing the agricultural processes (E2), respectively. The latter derived the monthly emission factors and activity data integrating the local information of soil, meteorology and agricultural processes. The total emissions were calculated at 1765 and 1067 Gg, respectively, and clear differences existed in seasonal and spatial distributions. Elevated emissions were found in March and September in E2, attributed largely to the increased top dressing fertilization and to the enhanced NH<sub>3</sub> volatilization under high temperature, respectively. Relatively large discrepancy between the inventories existed in northern YRD with abundant croplands. With the estimated emissions 38% smaller in E2, the average of simulated NH<sub>3</sub> concentrations with an air quality model using E2 were 27% smaller than those using E1 at two ground sites in YRD. At the suburban SHPD site, the simulated NH<sub>3</sub> concentrations with E1 were generally larger than observations, and the modeling performance was improved indicated by the smaller NMEs when E2 was applied. In contrast, very limited improvement was found at the urban site JSPAES, as E2 failed to improve the emission estimation of transportation and residential activities. Compared to NH<sub>3</sub>, the modeling performance for inorganic aerosols was better for most cases, and the differences between the simulated concentrations with E1 and E2 were clearly smaller, at 7%, 3% and 12% (relative to E1) for NH<sub>4</sub><sup>+</sup>, SO<sub>4</sub><sup>2-</sup>, and NO<sub>3</sub><sup>-</sup>, respectively. Compared to the satellite-derived NH<sub>3</sub> column, application of E2 significantly corrected the overestimation in vertical column density for January and October with E1, but did not improve the model performance for July. The NH<sub>3</sub> emissions might be underestimated with the assumption of linear correlation between NH<sub>3</sub> volatilization and soil pH for acidic soil, particularly in warm seasons. Three additional cases, i.e., 40% abatement of SO<sub>2</sub>, 40% abatement of NO<sub>x</sub>, and 40% abatement of both species were applied to test the sensitivity of NH<sub>3</sub> and inorganic aerosol concentrations to precursor emissions. Under an NH<sub>3</sub>-rich condition, estimation of SO<sub>2</sub> emissions was detected to be more effective on simulation of secondary inorganic aerosols compared to NH<sub>3</sub>. Reduced SO<sub>2</sub> would restrain the formation of (NH<sub>4</sub>)<sub>2</sub>SO<sub>4</sub>, and thereby enhance the NH<sub>3</sub> concentrations. To improve the air quality more effectively and

删除的内容: integrated the detailed information of soil, meteorology and agricultural processes, and

删除的内容: information of

删除的内容: , and agricultural activities (livestock farming and fertilizer use) were estimated to contribute 74-84% to total emissions in the two inventories.

删除的内容: C

删除的内容: of NH<sub>3</sub> emissions

删除的内容: methods

删除的内容: Yangtze River Delta

删除的内容: The two inventories were evaluated through air quality modeling and available ground and satellite observation.

删除的内容: was

删除的内容: that

删除的内容: observation

删除的内容: the

删除的内容: region

删除的内容: largely

删除的内容: local sources including

删除的内容: Regarding

删除的内容: simulation

删除的内容: for most of YRD

删除的内容: Besides the emissions, uncertainties existed as well in the limitations of ground and satellite observation and incomplete mechanism of gas to particle conversion applied in the model.

87 efficiently, NH<sub>3</sub> emissions should be substantially controlled along with SO<sub>2</sub> and NO<sub>x</sub>  
88 in the future.

89

90

## 1. Introduction

91 As the most important alkaline composition in the atmosphere, ammonia (NH<sub>3</sub>)  
92 exerts crucial influences on atmospheric chemistry and nitrogen cycle. NH<sub>3</sub>  
93 participates in chemical reactions with ~~sulphuric acid (H<sub>2</sub>SO<sub>4</sub>) and nitric acid (HNO<sub>3</sub>)~~  
94 and contributes to formation of secondary inorganic aerosols (SIA) including sulfate  
95 (SO<sub>4</sub><sup>2-</sup>), nitrate (NO<sub>3</sub><sup>-</sup>), and ammonium (NH<sub>4</sub><sup>+</sup>) and to thereby the elevated  
96 concentrations of fine particulate matters (PM). In the developed regions in eastern  
97 China, for example, SIA was observed to account for over 50% of PM<sub>2.5</sub> mass  
98 concentrations (Yang et al., 2011; Zhang et al., 2012; Huang et al., 2014), and NH<sub>3</sub>  
99 emissions were estimated to contribute 8-11% of PM<sub>2.5</sub> (Wang et al., 2011). Recent  
100 studies reported that existence of NH<sub>3</sub> could accelerate the heterogeneous oxidation of  
101 SO<sub>2</sub> and thereby sulfate formation by neutralizing aerosol acidity (Wang et al., 2016;  
102 Cheng et al., 2016; Paulot et al., 2017). Deposition of gaseous NH<sub>3</sub> and NH<sub>4</sub><sup>+</sup> aerosols  
103 results in soil acidification and water eutrophication. Reduced nitrogen (NH<sub>3</sub>+NH<sub>4</sub><sup>+</sup>)  
104 was monitored to contribute over 70% of total nitrogen deposition in China, revealing  
105 the importance of NH<sub>3</sub> on ecosystem (Pan et al., 2012). ~~Recently the SO<sub>2</sub> and NO<sub>x</sub>~~  
106 ~~emissions have gradually decreased due to implementation of air pollution control~~  
107 ~~measures in China, thus,~~ NH<sub>3</sub> emissions ~~were~~ found to ~~play a greater role on~~ secondary  
108 aerosol formation and nitrogen deposition ~~compared to previous years~~ (Liu et al.,  
109 2013; Fu et al., 2017; Pan et al., 2018).

110 Quantification of NH<sub>3</sub> sources helps better understanding its atmospheric and  
111 ecosystem effects. In contrast to SO<sub>2</sub> and NO<sub>x</sub> that are largely from industrial plants,  
112 NH<sub>3</sub> comes mainly from agricultural activities that are more difficult to track,  
113 including livestock farming and fertilizer use, and relatively large uncertainty in NH<sub>3</sub>  
114 emission inventories existed. Given the intensive agriculture across the country,  
115 various methods were developed to estimate China's NH<sub>3</sub> emissions at the national  
116 level for last twenty years, but clear discrepancies existed between studies, as  
117 summarized by Zhang et al. (2018). With meteorology, soil property, the method of  
118 fertilizer application and different processes of manure management considered in  
119 emission factor (emissions per unit level of activity) determination, in particular, the

删除的内容: sulfur dioxide (SO<sub>2</sub>)

带格式的: 下标

带格式的: 下标

删除的内容: nitrogen oxides (NO<sub>x</sub>),

带格式的: 下标

删除的内容: Along with

带格式的: 下标

删除的内容: the improved controls of  
SO<sub>2</sub> and NO<sub>x</sub> emissions, enhanced  
contribution of

删除的内容: was

删除的内容: for recent years in China

128 national NH<sub>3</sub> emissions estimated by Peking University group (Huang et al., 2012;  
129 Kang et al., 2016) was 39-46% smaller than those by Tsinghua University group  
130 (Dong et al., 2010; Zhao et al., 2013). Emissions of certain sectors differed  
131 significantly between various methods. For example, Zhao et al. (2013) and  
132 Kurokawa et al. (2013) calculated China's NH<sub>3</sub> emissions from fertilizer use at 9.5-9.8  
133 Tg, over three times of the estimation by Kang et al. (2016). With a fertilizer  
134 modeling system that couples an air quality model and an agro-ecosystem model, Fu  
135 et al. (2015) made an estimate at 3.0 Tg, similar with Kang et al. (2016). Besides the  
136 annual emission level, discrepancies existed as well in the inter-annual trend of  
137 emissions. Kang et al. (2016) estimated that the national NH<sub>3</sub> emissions reached the  
138 peak in 1996 and declined thereafter, while Zhang et al. (2017) and Kurokawa et al.  
139 (2013) expected a continuous growth till 2008 and 2015, respectively. The growth in  
140 NH<sub>3</sub> emissions got supported by satellite observation. Based on the measurement of  
141 Atmospheric Infrared Sounder (AIRS), for example, Warner et al. (2017) suggested an  
142 annual increasing rate of NH<sub>3</sub> concentrations at 2.3% from 2002 to 2016 in China, and  
143 it was partly attributed to the elevated emissions from fertilizer use.

144 Although varied methods and data resulted in discrepancies between inventories  
145 and big uncertainty in NH<sub>3</sub> emission estimation, very little attention has been paid to  
146 those discrepancies and the underlying reasons. At the regional scale, in particular,  
147 inclusion of high-resolution information on meteorology and land use would  
148 potentially improve the spatial and seasonal distribution of agricultural NH<sub>3</sub> emissions  
149 in the inventory. Previous studies have demonstrated that including meteorology field  
150 could improve NH<sub>3</sub> emission estimation for both Europe and North America  
151 compared to simple static methodology (Bash et al., 2013; Gyldenkaerne et al., 2005;  
152 Skjoeth et al., 2011; Wichink Kruit et al., 2012), while the inter-comparison studies  
153 have not sufficiently been conducted for China. Moreover, few studies were  
154 conducted to evaluate NH<sub>3</sub> emission inventories incorporating air quality model and  
155 available ground and satellite observations. One possible reason is the lack of  
156 sufficient ground observation data on NH<sub>3</sub> and NH<sub>4</sub><sup>+</sup> aerosols open to public, as they  
157 are currently not regulated air pollutants in China and thus not regularly monitored by  
158 the government. In addition, uncertainty also existed in satellite observation on NH<sub>3</sub>  
159 columns and the retrieved data needs further validation (van Damme et al., 2015).  
160 Without comparison of different inventories in details and appropriate assessment  
161 based on model performance, the limitations of current emission estimates and the

删除的内容: carefully

163 future steps for inventory improvement remained unclear.

164 In this study, therefore, we chose the Yangtze River Delta (YRD) region to  
165 develop and evaluate the emission inventories of NH<sub>3</sub> with different methods and data  
166 sources. Located in eastern China, the YRD region contains the city of Shanghai and  
167 the provinces of Jiangsu, Zhejiang and Anhui (see Figure 1 for its location and  
168 prefectural cities), and is one of China's most developed and heavy-polluted regions  
169 (Xiao et al., 2011; Cheng et al., 2013; Guo et al., 2017). It is an important area of  
170 agriculture production, and was identified as a "NH<sub>3</sub>-rich" region regarding the SIA  
171 formation (Wang et al., 2011). We developed two NH<sub>3</sub> emission inventories for 2014  
172 based on the constant emission factors (E1) and those characterizing the agricultural  
173 processes (E2), respectively. The two inventories were compared against each other to  
174 reveal the differences in spatial and seasonal patterns of NH<sub>3</sub> emissions and their  
175 origins. Evaluation of the two inventories was further conducted using a Models-3  
176 Community Multi-scale Air Quality (CMAQ) system and available observations from  
177 ground station and satellite. Environmental parameters that might influence NH<sub>3</sub>  
178 simulation were identified through the model performance. Finally, the effects of SO<sub>2</sub>  
179 and NOx emission estimates on NH<sub>3</sub> and NH<sub>4</sub><sup>+</sup> aerosol simulation were evaluated  
180 through sensitivity analysis, and the policy implication of air quality improvement  
181 were accordingly suggested.

删除的内容: high-resolution

删除的内容: the

删除的内容: Method

删除的内容: Method

182

## 183 2. Data and methods

### 184 2.1 Emission inventory based on the constant emission factors (E1)

185 The annual NH<sub>3</sub> emissions of the YRD region for 2014 were estimated with a  
186 bottom-up method based on the constant emission factors, and then allocated to the  
187 monthly level based on the previously investigated temporal profile of emissions. The  
188 inventory contained eight source categories, i.e., fertilizer application,  
189 livestock/poultry breeding, fuel combustion, biomass burning, transportation,  
190 sewage/waste treatment, industrial process, and human metabolism (see Table 1 for  
191 the details). Note that the emissions from pets were not included in the current work,  
192 due to lack of detailed information. Given their relative small fraction in total  
193 emissions, e.g., less than 2% in United Kingdom (Sutton et al., 1999; 2000), we  
194 believed that the uncertainty was limited. The annual emissions were calculated by  
195 prefectural city with the Eq. 1:

删除的内容: .

201 
$$E_i = \sum_j (AL_{i,j} \times EF_j \times 10^{-3}) \quad (1)$$

删除的内容:

202 where  $E$  is the emissions, metric ton (t);  $i$  and  $j$  indicate the prefectural city and source  
203 type, respectively;  $AL$  is the activity level, which indicated the amount of livestock,  
204 the amount of used fertilizer, the fuel burned or the industrial production, depending  
205 on the source type; and  $EF$  is the annual emission factor, kg-NH<sub>3</sub>/unit  $AL$ .

206 The activity data were mainly taken or estimated from official statistics at the  
207 prefectural city (if available) or provincial level. For livestock/poultry breeding, the  
208 year-end stock and slaughtered numbers were used respectively for animals with the  
209 breeding cycle more and less than one year. If the city-level stock was unavailable, the  
210 output of livestock products by prefectural city was applied as the scaling factor to  
211 calculate the number from the provincial data. Table S1 in the supplement summarizes  
212 the annual numbers of livestock and poultry by prefectural city in YRD. The amount  
213 of fertilizer used by prefectural city and type was calculated as the product of sown

删除的内容: A

214 area of cropland and fertilizer rate per unit area of cropland. The sown area by crop  
215 type was taken from city-level statistics, and the application rate by fertilizer type was  
216 obtained at provincial level from a national investigation by NDRC (2015). The  
217 detailed results of fertilizer activity data are summarized in Table S2 in the  
218 supplement. As can be seen as well in the table, the aggregated amount of fertilizer  
219 used by province was close to the provincial-level statistics, and the deviation relevant  
220 to the official statistics was 2.3% for the whole YRD. The methods and data sources  
221 for activity levels of other source categories were provided in our previous studies  
222 (Zhou et al., 2017; Zhao et al., 2017; Yang and Zhao, 2019).

删除的内容: ing

223 The annual NH<sub>3</sub> emission factors were obtained based on a thorough literature  
224 review and summarized by source category in Table S3 in the supplement. The results  
225 from domestic field measurements were preferentially selected. For sources without  
226 suitable domestic measurements, the emission factors were also obtained from  
227 previous inventories that shared similar studying period with this work. The values  
228 from US and Europe, e.g., AP-42 database (USEPA, 2002) and the EMEP/EEA  
229 guidebook (EEA, 2013a; b), were adopted, when above information was lacking.

删除的内容: using

删除的内容: were

230 The monthly distribution of emissions by source was taken from domestic  
231 investigations in YRD (Li, 2012; Zhao et al., 2015; Zhou et al., 2017). For the purpose  
232 of air quality modeling, the emissions by sector were allocated into a grid system with  
233 a horizontal resolution at 9×9 km based on selected proxies. Those proxies included

删除的内容: 2013

删除的内容: as well



241 the distribution of land use (for fertilization), density of total population (for human  
242 metabolization and sewage/waste treatment) and rural population (for  
243 livestock/poultry breeding and residential solid fuel burning), gross domestic product  
244 (for industrial fuel combustion and processes), road net (for transportation), and the  
245 satellite-derived fire points from Moderate Resolution Imaging Spectroradiometer (for  
246 open biomass burning, [Davies et al., 2009](#)).

## 247 2.2 The method characterizing the agricultural processes (E2)

248 The emissions from fertilizer use and livestock/poultry breeding were  
249 recalculated integrating the detailed regional information of soil, meteorology and  
250 agricultural processes. The same annual activity data as E1 (e.g., livestock/poultry  
251 numbers in Table S1 and fertilizer used in Table S2) were applied.

### 252 2.2.1 Fertilizer use

253 The growing seasons of crops affects the temporal distribution of fertilizer use  
254 and thereby that of NH<sub>3</sub> emissions. We investigated the growing and farming cycles  
255 by crop type in YRD from the regional farming database by the Ministry of  
256 Agriculture (MOA, <http://202.127.42.157/moazzys/nongshi.aspx>) and other  
257 publication (Zhang et al., 2009). Taking the early-season rice as an example, the basal  
258 dressing was usually conducted in mid-April, with all the complex-fertilizer and half  
259 of the other nitrogen fertilizer used. The top dressing was conducted three times, i.e.,  
260 10% and 10% of nitrogen fertilizer used 7 days and 14 days after transplanting, and  
261 the left 30% used for sprouting, respectively. With that information incorporated, we  
262 estimated the monthly amount of fertilizer usage by prefectural city and fertilizer type  
263 based on the annual amount in Table S2.

264 Emission factors of fertilization were expected to be influenced by soil acidity,  
265 temperature, and the fertilization rate. We assumed a linear correlation between the  
266 soil pH and NH<sub>3</sub> volatilization rate (Huang et al., 2012), and calculated the monthly  
267 emission factors of two fertilization types (basal dressing and top dressing) with Eq. 2  
268 and 3, respectively:

$$269 EF_{basal} = [(a_{pH} \times pH + b_{pH}) + (T_{basal} - T_0) \times k_T] \times CF_{rate} \times CF_{method} \quad (2)$$

$$270 EF_{top} = [(a_{pH} \times pH + b_{pH}) + (T_{top} - T_0) \times k_T] \times CF_{rate} \quad (3)$$

271 where  $EF_{basal}$  and  $EF_{top}$  are the emission factors for basal dressing and top dressing,  
272 respectively;  $a_{pH}$  and  $b_{pH}$  are the slope and intercept depending on soil pH;  $T_0$  and  $k_T$

删除的内容: Method

删除的内容: corrected or

删除的内容: , as described below.

删除的内容: , and

删除的内容: corrected

删除的内容: using

删除的内容: combining

删除的内容: the information of farming season and

删除的内容: fertilizer using as given

删除的内容: .

删除的内容: near-

删除的内容:

删除的内容:

删除的内容: corrected



288 are the reference temperature and the slope depending on temperature, respectively;  
289  $T_{basal}$  and  $T_{top}$  are the monthly average temperature of basal dressing and top dressing,  
290 respectively; and  $CF_{rate}$  and  $CF_{method}$  are the correction factors for fertilization rate and  
291 application method (basal dressing), respectively.

删除的内容: corrected

删除的内容: corrected

删除的内容: .

292 The spatial distribution of soil pH at a horizontal resolution of 1×1km was  
293 obtained from a world soil database by International Institute for Applied Systems and  
294 Analysis (IIASA,  
295 <http://webarchive.iiasa.ac.at/Research/LUC/External-World-soil-database/HTML/>).

删除的内容:

带格式的: 缩进: 首行缩进: 0.85 厘米

296 The correlation data between temperature and  $NH_3$  volatilization rate were obtained  
297 from EEA (2009).  $T_{basal}$  and  $T_{top}$  were determined combining the information of  
298 farming season by MOA and the daily temperature data from European Centre for  
299 Medium-Range Weather Forecasts (ECMWF,  
300 <http://apps.ecmwf.int/datasets/data/interim-full-daily/levtype=sfc/#userconsent#>). All

删除的内容: 2013

删除的内容: ECNWF

301 the relevant data for emission factor correction were summarized in Table S4 in the  
302 supplement. The monthly  $NH_3$  volatilization rates of urea and ammonium bicarbonate  
303 (ABC), the mostly applied two types of fertilizer over the YRD region, were  
304 illustrated by season in Figure S1 in the supplement. Larger volatilization rates were  
305 found in northern YRD for both fertilizer types, consistent with the distribution of soil  
306 pH across the region. Taking urea as an example, the volatilization rates in April and  
307 October were commonly smaller than the uniform value applied in E1 at 17.4%, while  
308 those in July were larger. This discrepancy came partly from the consideration of  
309 fertilization types in E2. In April and October, basal dressing fertilization was  
310 commonly applied at the soil depth of 15-20 centimeters, restraining the  $NH_3$   
311 volatilization. In contrast, the relatively high temperature and top dressing fertilization  
312 conducted in July elevated the  $NH_3$  volatilization. It should be noted that the local  
313 fertilizer application introduced some bias to the soil pH from the global database by  
314 IIASA. Basal dressing would increase the soil pH (particularly for the acidic soils) as  
315 indicated in previous domestic study (Zhong et al., 2006). Due to lack of the  
316 quantitative relation between the fertilizer application and soil pH at the regional scale  
317 in China, we ignored the interaction between the them in Eqs.(2).

删除的内容: corrected

带格式的: 非上标/ 下标

带格式的: 字体: Times New Roman

带格式的: 字体: Times New Roman

带格式的: 字体: Times New Roman

带格式的: 字体: Times New Roman

318 Through the methodology mentioned above, the gridded emission factors and  
319 monthly activity levels were obtained to improve the spatial and temporal  
320 distributions of  $NH_3$  emissions from fertilization. Figure 2 compares the spatial

删除的内容: .

329 | ~~distribution of the monthly fertilizer usage~~ between ~~E1~~ and ~~E2~~, indicated by the  
330 | relative deviation (*RD*):

$$331 \quad RD = (E_1 - E_2)/(E_1 + E_2)/2 \quad (4)$$

332 | In January and July, top dressing fertilization was conducted with limited crop types  
333 | like rape, corn and paddy rice, while considerable basal dressing fertilization was  
334 | investigated in April and October. Inclusion of those details in E2 resulted in smaller  
335 | estimates of fertilizer use in winter and summer but larger in spring and autumn  
336 | compared to E1.

### 337 | 2.2.2 Livestock/poultry breeding

338 | In contrast to ~~E1~~ that calculated the NH<sub>3</sub> emissions based on livestock numbers  
339 | and annual EFs, a mass-flow approach was applied in ~~E2~~ considering the nitrogen  
340 | transformation at different stages of manure management (Beusen et al., 2008; ~~EEA~~,  
341 | ~~2013a~~; Huang et al., 2012). Commonly applied at ~~the~~ global or national scale, the  
342 | approach calculated NH<sub>3</sub> emissions of manure management processes from a pool of  
343 | total ammoniacal nitrogen (TAN) for three main raising systems, as shown in Figure  
344 | S2 in the supplement. In ~~the~~ YRD region, only intensive and free-range systems were  
345 | considered, and the TAN was calculated by livestock/poultry type based on the  
346 | breeding duration, the amount and nitrogen contents of urine/feces, and the mass  
347 | fraction of TAN. The parameters were taken from Yang (2008) and Huang et al (2012),  
348 | as summarized in Table S5 in the supplement. According to the nitrogen flow and  
349 | phase of manure management, the activity levels were then classified into seven  
350 | categories, including outdoor, housing (solid), housing (liquid), storage (solid),  
351 | storage (liquid), spreading (solid) and spreading (liquid). NH<sub>3</sub> emissions from  
352 | livestock are calculated as the product of TAN of each category and corresponding  
353 | emission factors. As provided in Table S6 in the supplement, the  
354 | temperature-dependant emission factors by stage/phase were taken from ~~Huang et al.~~  
355 | (2012), and the gridded emission factors can then be derived over the YRD region  
356 | combining the meteorology data from ~~ECMWF~~.

357

### 358 | 2.3 Configuration of air quality modeling

359 | The Models-3 Community Multi-scale Air Quality (CMAQ) version 4.7.1 was  
360 | applied to evaluate the NH<sub>3</sub> emission inventories for YRD. CMAQ is a  
361 | three-dimensional Eulerian model designed for understanding the complex

删除的内容: activity dat

删除的内容: a of fertilization

删除的内容: the two methods (

删除的内容: )

删除的内容: Method

删除的内容: Method

删除的内容: ; EEA, 2013

删除的内容: EEA (2013) and

删除的内容: ECNWF

371 | interactions of atmospheric chemistry and physics ([UNC, 2010](#)). The model has been  
372 | widely applied and tested in China (Qin et al., 2015; Zhou et al., 2017; Zheng et al.,  
373 | 2019). As shown in Figure 1, two nested domains were applied with the spatial  
374 | resolutions of 27 and 9 km respectively, on a Lambert Conformal Conic projection  
375 | centered at (110°E, 34°N). The mother domain (D1, 177×127 cells) covered most  
376 | parts of China, and the second domain (D2, 118×121 cells) covered the whole YRD  
377 | region. The two inventories of YRD NH<sub>3</sub> emissions developed in this work were  
378 | applied in D2. Emissions from other pollutants of anthropogenic origin in D1 and D2  
379 | outside Jiangsu were obtained from the Multi resolution Emission Inventory for China  
380 | (MEIC, <http://www.meicmodel.org/>) with an original spatial resolution of 0.25°×0.25°.  
381 | Population density was applied to relocate MEIC to each modeling domain. A  
382 | high-resolution inventory that incorporates more information of local emission  
383 | sources was applied for Jiangsu (JS, Zhou et al., 2017). Both MEIC and JS inventories  
384 | are for 2012. The emissions for 2014 were obtained using a simple scaling method  
385 | based mainly on changes in activity levels (e.g., energy consumption and industrial  
386 | production) between the three years. Biogenic emission inventory was from the  
387 | Model Emissions of Gases and Aerosols from Nature 2.1 (MEGAN2.1, [Guenther et](#)  
388 | [al., 2012](#); [Sindelarova et al., 2014](#)), and the emission inventories of Cl, HCl and  
389 | lightning NO<sub>x</sub> were from the Global Emissions Initiative (GEIA, Price et al., 1997).  
390 | Meteorological fields were provided by the Weather Research and Forecasting Model  
391 | (WRF) version 3.4, a state-of-the-art atmospheric modeling system designed for both  
392 | meteorological research and numerical weather prediction ([Skamarock et al., 2008](#)),  
393 | and the carbon bond gas-phase mechanism (CB05) and AERO5 aerosol module were  
394 | adopted. Other details on model configuration and parameters were given in Zhou et  
395 | al. (2017). The simulations were conducted for January, April, July and October to  
396 | represent the four typical seasons in 2014. A 5-day spin-up period of each month was  
397 | used to minimize the influences of initial conditions in the simulations.

398 | Using the observation data of US National Climate Data Center (NCDC) at 43  
399 | stations in YRD (see Figure 1 for the locations of the stations), the WRF modeling  
400 | performance was evaluated with statistical indicators including averages of  
401 | simulations and observations, bias, normalized mean bias (NMB), normalized mean  
402 | error (NME), root mean squared error (RMSE) and index of agreement (IOA). As can  
403 | be found in Table S7 in the Supplement, discrepancies between simulation and

删除的内容: <http://www.cmaq-model.org>

删除的内容: , etc

带格式的: 字体: Times New Roman

带格式的: 字体: Times New Roman

删除的内容: <http://www2.mmm.ucar.edu/wrf/users/>

409 observation met the criteria by Emery et al. (2001) for most cases, implying the  
410 reliability of meteorological simulation. However, bigger errors were found for the  
411 simulation of wind direction.

#### 412 **2.4 Ground-based and satellite observations**

413 There were very limited continuous ground measurement data available for  
414 ambient  $\text{NH}_3$  and  $\text{NH}_4^+$  aerosol in the YRD region 2014, particularly at rural/remote  
415 sites that are more representative for the regional atmospheric environment. We  
416 conducted on-line hourly measurements using the MARGA (Monitor for AeRosols  
417 and Gases in ambient Air, ADI2080) at an urban site in the western downtown of  
418 Nanjing (32.03°N, 118.44°E) from August 2014. The MARGA is a state-of-art  
419 instrument which monitors near real-time water-soluble ions in aerosols and their  
420 gaseous precursors (Lanciki, 2018), and it was able to capture rapid compositional  
421 changes in  $\text{PM}_{2.5}$  (Chen et al., 2017). The site was on the roof of the building of  
422 Jiangsu Provincial Academy of Environmental Science (30 m above the ground)  
423 surrounded by residential and commercial buildings and heavy traffic (JSPAES: Li et  
424 al., 2015; Chen et al., 2019). The data of October 2014 were applied in this work to  
425 evaluate the  $\text{NH}_3$  inventories through air quality simulation. Besides, the hourly data  
426 of online measurement with MARGA were available at a suburban site in Pudong,  
427 Shanghai (SHPD) for April, July and October 2014 (unpublished data from Shanghai  
428 Environmental Monitoring Center).

429 Regarding satellite observation, the daily  $\text{NH}_3$  vertical column densities (VCDs)  
430 measured through Infrared Atmospheric Sounding Interferometer (IASI) were  
431 downloaded from ESPRI data center  
432 (<http://cds-espri.ipsl.upmc.fr/etherTypo/index.php?id=1700&L=1>). We used the data  
433 in the domain (114.2°E-124.1°E, 26.1°N-35.4°N) with a 9:30am equator local  
434 crossing time to evaluate the  $\text{NH}_3$  emissions. Only pixels with radiative cloud  
435 fraction < 25%, relative error < 100% and absolute error <  $5 \times 10^{15}$  molec/cm<sup>2</sup> were used  
436 following the criteria of previous studies (van Damme et al., 2014; 2015). The  
437 monthly average VCDs for January, April, July and October 2014 were calculated and  
438 allocated into a grid system of 0.5° (longitude) × 0.25° (latitude) using the Kriging  
439 interpolation method, as shown in Figure 3.

440

### 3. Results and discussions

#### 3.1 Comparison between the two inventories

Table 2 summarizes the NH<sub>3</sub> emissions estimated with E1 and E2 by source category and province for the YRD region in 2014. Agricultural activities (livestock farming and fertilizer) were identified as the most important sources of NH<sub>3</sub>, with the fraction to total emissions ranged 74-84% in the two methods. Applying the constant emission factors, E1 derived a total NH<sub>3</sub> emission estimate 60% larger than that by E2 that characterized the agricultural processes. In particular, emissions from agricultural activities in E1 were calculated as twice of those in E2. At the national scale, similarly, Dong et al. (2016) applied the constant emission factors and estimated the total NH<sub>3</sub> emissions at 16.1 Tg for China, 64% larger than 9.8 Tg by Huang et al. (2012) with the agricultural processes characterized. The clearly larger estimation by constant emission factors was due partly to the fact that most domestic measurements, on the emission factors of NH<sub>3</sub> from fertilizer application were conducted in hot seasons (late spring and summer), when the basal dressing of single-season rice and maize and top dressing of wheat were usually conducted (Cai et al., 2002; Huo et al., 2015; Su et al., 2006). However, the crop rotation varied a lot in China, and part of the nitrogen fertilizer was actually not applied in hot seasons. Emission estimation based on those emission factors may thus overestimate the NH<sub>3</sub> emission intensity (Huo et al., 2015; Wang et al., 2011; Zhang et al., 2010). Among the provinces, the fraction of Jiangsu to YRD emissions was ranged 45-47% in the two methods, followed by Anhui around 37%. Agricultural activities were relatively intensive in the two provinces: Jiangsu and Anhui contributed 46% and 33% of the economic output of agriculture and livestock/poultry farming in YRD, and the collective fraction of fertilizer use by the two provinces reached 84%. In contrast, agricultural activities were limited in Shanghai and Zhejiang, with smaller emissions estimated in both inventories.

The monthly distribution of NH<sub>3</sub> emissions in the two inventories were illustrated in Figure 4. Both inventories indicated the relatively large emissions in summer (from June to August), and the elevated emissions were also found in March and September in E2. The difference comes mainly from the effect of farming season on fertilization process. For example, the top dressing fertilization for winter wheat was conducted mostly during the seedling establishment and elongation stage in the following spring, resulting in enhanced use of nitrogen fertilizer in March. Moreover,

- 删除的内容: mainly
- 删除的内容: emission factor
- 删除的内容:
- 带格式的
- 带格式的: 下标
- 带格式的
- 带格式的
- 带格式的
- 带格式的: 字体: Times New Roman
- 带格式的: 字体: Times New Roman
- 带格式的
- 删除的内容: .
- 带格式的
- 带格式的
- 带格式的: 字体: Times New Roman
- 带格式的
- 带格式的: 字体: Times New Roman
- 带格式的: 字体: Times New Roman
- 带格式的: 字体: Times New Roman
- 带格式的: 下标
- 删除的内容:
- 删除的内容: region
- 删除的内容: M

481 September was the month with the highest temperature following summer in YRD  
482 2014, and the elevated NH<sub>3</sub> volatilization led to large emissions in E2. Compared to  
483 the fertilizer use, less variation of monthly emissions were found for livestock/poultry  
484 breeding, as very limited change in livestock amount was detected in both inventories.

485 Illustrated in Figure 5 are the spatial distributions of emissions from fertilizer use,  
486 livestock/poultry breeding and all categories in the two inventories. Both inventories  
487 indicated the large emission intensities in northern Jiangsu (Xuzhou and Yancheng)  
488 and northern Anhui (Fuyang, Bozhou and Suzhou) with abundant agricultural  
489 production. Xuzhou and Yancheng collectively contributed 36%, 31% and 41% of the  
490 provincial fertilizer use, agricultural economic product, and livestock/poultry farming  
491 product in Jiangsu, respectively. Similarly, Fuyang, Bozhou and Suzhou collectively  
492 contributed 36%, 36% and 35% of the provincial sown area, agricultural economic  
493 product, and livestock/poultry farming product in Anhui, respectively.

494 The differences in spatial pattern between the two inventories were further  
495 investigated for total and fertilizer use emissions by month, through the indicator *RD*  
496 calculated with Eq. (4). As shown in Figure 6, larger *RD* was found in northern  
497 Jiangsu, northern Anhui, and eastern Zhejiang, while smaller in western Zhejiang. The  
498 emissions in E1 were commonly larger than that in E2 across the YRD region for  
499 January and April. In contrast, larger emissions in E2 were found in northern Jiangsu  
500 (e.g., Xuzhou and Yancheng) and northern Anhui for July and October. The  
501 discrepancy resulted from the combined effect of varied activity data and emission  
502 factors as described in Section 2.2: top dressing fertilization and high temperature led  
503 to enhanced volatilization rate and thereby emissions of NH<sub>3</sub> in E2, and the abundant  
504 fertilizer use in the broad cropland in northern YRD, was the main reason for the high  
505 emissions in October.

506 Figure 7 compares the NH<sub>3</sub> emissions by province and source category in this  
507 work and other available downscaled national (MEIC) or provincial inventories in the  
508 YRD region. Results from other studies were commonly ranged between E1 and E2  
509 for agriculture, the most important NH<sub>3</sub> source. With the constant emission factors  
510 applied, the MEIC estimates were similar to those in E1. Most current provincial  
511 inventories made some corrections for emissions from fertilizer use or  
512 livestock/poultry breeding, but the local geographical and meteorological information  
513 was seldom applied in the emission estimation. For example, Liu and Yao (2016)  
514 calculated the emissions from livestock/poultry breeding for Jiangsu based on TAN,

删除的内容: region

删除的内容: were

删除的内容: not always fully

518 but did not consider the impacts of varied monthly temperatures on the emissions.  
519 Zheng et al. (2016) calculated the agricultural NH<sub>3</sub> emissions for Anhui based on a  
520 national guideline of NH<sub>3</sub> emission inventory development (MEP, 2014), and ignored  
521 the impact of soil condition (e.g., pH) on NH<sub>3</sub> volatilization from fertilizer use.

### 522 **3.2 Evaluation of the inventories with transport modeling and ground** 523 **observation**

524 Figures 8 illustrates the observed and simulated hourly concentrations for  
525 gaseous NH<sub>3</sub> and inorganic aerosol species (NH<sub>4</sub><sup>+</sup>, SO<sub>4</sub><sup>2-</sup> and NO<sub>3</sub><sup>-</sup>) in PM<sub>2.5</sub> for April,  
526 July and October at SHPD and October at JSPAES. The normalized mean biases  
527 (NMB) and normalized mean errors (NME) between observed and simulated  
528 concentrations, and the monthly average concentrations from observation and  
529 simulation are summarized in Table 3. The simulated monthly average concentrations  
530 were close to the observed ones at both sites. The biggest discrepancy was found at  
531 SHPD for April, where the monthly average NH<sub>3</sub> was simulated 56% larger than  
532 observation with E1, and the smallest at JSPAES for October, where the simulated  
533 was 1.7% smaller than observation with E1. The simulated temporal variation,  
534 however, was much larger than the observation, leading to relatively large NME,  
535 particularly at SHPD for April. Clear difference was found for the simulation under  
536 two NH<sub>3</sub> inventories. In general, the average of simulated NH<sub>3</sub> concentrations at the  
537 two sites for available months was 27% smaller in E2 than that in E1 (note the total  
538 NH<sub>3</sub> emissions in E2 was 38% smaller than that in E1 for the whole YRD region). At  
539 SHPD site, application of E1 in CMAQ overestimated the NH<sub>3</sub> concentration,  
540 indicated by the positive NMB values and the larger simulated concentrations than  
541 observation. Such overestimation was corrected when E2 was applied, and the NMEs  
542 with E2 were substantially reduced as well, as shown in Table 3. The better modeling  
543 performance implies the improved estimation and spatiotemporal distribution of  
544 emissions. At JSPAES, the air quality modeling with both inventories underestimated  
545 the NH<sub>3</sub> concentrations, and the simulated monthly average concentration with E1  
546 was much closer to observation than that with E2. The close NMEs between the two  
547 inventories indicated very limited improvement at the site, in contrast to SHPD.  
548 Located in urban area, JSPAES might be largely affected by the local sources like  
549 transportation and residential activities. NH<sub>3</sub> emissions of such source categories,  
550 however, were not improved in E2.

删除的内容: ambient particles

带格式的: 下标

删除的内容: clearly



553 To reduce the impact of the highly uncertain hourly meteorology simulation and  
554 emission data on air quality modeling, the daily NH<sub>3</sub> concentrations derived from  
555 simulation and observation were further compared for October at JSPAES. As  
556 illustrated in Figure S3 in the supplement, better agreement between observation and  
557 simulation was achieved for the daily concentrations than the hourly, and the NMEs  
558 for E1 and E2 were reduced respectively from 56.9% and 53.7% to 37.0% and 32.5%,  
559 respectively. Besides the emission data, uncertainty in meteorology simulation also  
560 contributed to the discrepancy between simulation and observation. For example, both  
561 inventories overestimated the concentration on 7<sup>th</sup> October but underestimated that on  
562 21<sup>st</sup>-22<sup>nd</sup>. In contrast to the southeasterly wind observed at ground meteorology station  
563 in Nanjing, the simulated wind direction on 7<sup>th</sup> was from north, enhancing the NH<sub>3</sub>  
564 transport from Yancheng and Xuzhou in northern Jiangsu with intensive agricultural  
565 activities. On 21<sup>st</sup>-22<sup>nd</sup>, the underestimation NH<sub>3</sub> concentration resulted largely from  
566 the overestimation in wind speed by WRF.

删除的内容: for

删除的内容: and thereby emissions

567 Compared to NH<sub>3</sub>, the modeling performance for inorganic aerosols (NH<sub>4</sub><sup>+</sup>, SO<sub>4</sub><sup>2-</sup>,  
568 and NO<sub>3</sub><sup>-</sup>) is better for most cases, indicated by the smaller NMEs and larger  
569 correlation coefficients (r) in Table 3. Some exceptions exist at SHPD for NH<sub>4</sub><sup>+</sup> and  
570 SO<sub>4</sub><sup>2-</sup> in October and NO<sub>3</sub><sup>-</sup> in January. Application of E2 reduced the NMEs and  
571 improved the simulation of NH<sub>4</sub><sup>+</sup> and SO<sub>4</sub><sup>2-</sup> moderately, but there were no significant  
572 changes between the modeling results with E1 and E2. The averages of simulated  
573 concentrations at the two sites for available months was 7%, 3% and 12% smaller in  
574 E2 than those in E1 for NH<sub>4</sub><sup>+</sup>, SO<sub>4</sub><sup>2-</sup>, and NO<sub>3</sub><sup>-</sup>, respectively, and the differences were  
575 clearly smaller than that for NH<sub>3</sub> at 27%. As large fraction of inorganic aerosols  
576 comes from secondary chemistry reaction, they are more representative for the  
577 regional atmosphere condition other than the local environment around the  
578 measurement site. Therefore, the air quality modeling at a horizontal resolution at 9×9  
579 km is expected to be able to better simulate the concentrations for SIA than the  
580 primary gaseous pollutants, particularly when emissions from some local sources are  
581 not sufficiently quantified. The simulated concentrations were commonly larger than  
582 observation for NH<sub>4</sub><sup>+</sup> and SO<sub>4</sub><sup>2-</sup>, particularly at SHPD in July and October. The  
583 uncertainty of model could be an importance source of the discrepancy, as the recent  
584 reported mechanisms of gas to particle conversion were not sufficiently applied in the  
585 CMAQ we used (Wang et al., 2016; Cheng et al., 2016). In addition, positive or  
586 negative artifacts also existed in ground observation with MARGA, resulting from the

删除的内容: secondary inorganic aerosols



591 | unexpected reaction between acid gaseous pollutants and nitrate aerosol ([Chen et al.](#)  
592 | [2017](#); [Schaap et al., 2011](#); [Stieger et al., 2018](#); Wei et al., 2015). From an emission  
593 | perspective, the overestimation was partly corrected when smaller NH<sub>3</sub> emissions in  
594 | E2 were applied instead of E1 in the model. Due to missing information on individual  
595 | industrial plants, moreover, the inventory we used in CMAQ failed to fully capture  
596 | the progress of emission control in [the](#) YRD region and probably overestimated the  
597 | SO<sub>2</sub> emissions (Zhang et al., 2019). The formation of sulfate ammonium aerosols  
598 | could then be enhanced through the irreversible reaction between SO<sub>2</sub> and NH<sub>3</sub>. The  
599 | process simultaneously reduced the amount of NH<sub>3</sub> reacted with HNO<sub>3</sub>, leading  
600 | further to the underestimation of nitrate aerosols. As shown in Table 3, application of  
601 | E2 with less NH<sub>3</sub> emissions than E1 could not improve the modeling performance of  
602 | nitrate aerosols. The impact of SO<sub>2</sub> and NO<sub>x</sub> emission on SIA modeling will be  
603 | further discussed in Section 3.4.

### 604 | **3.3 Evaluation of the inventories with transport modeling and satellite** 605 | **observation**

606 | To be consistent with the local crossing time of IASI at 9:30am, the average of  
607 | simulated hourly NH<sub>3</sub> concentrations at 9:00 am and 10:00 am were applied to  
608 | calculate the NH<sub>3</sub> VCDs, using the following equations:

$$609 \quad n_{\text{NH}_3} = \sum_{k=1}^{23} m_k \times \Delta H_k \times 100 \quad (5)$$

$$610 \quad \Delta H_k = H \times \ln\left(\frac{p_k}{p_{k+1}}\right) \quad (6)$$

611 | where  $n_{\text{NH}_3}$  is the NH<sub>3</sub> VCDs from CMAQ model (molec./cm<sup>2</sup>);  $m_k$  is the simulated  
612 | NH<sub>3</sub> concentrations at vertical layer  $k$  in the CMAQ (molec./cm<sup>3</sup>);  $\Delta H$  is the height of  
613 | layer  $k$  (m);  $H$  represents the height when the pressure of atmosphere declines to 1/e  
614 | of the original value; and  $p$  is the air pressure. Figure 9 illustrates the simulated NH<sub>3</sub>  
615 | VCDs with E1 and E2 for January, April, July, and October. Similar spatial patterns  
616 | are found with the two inventories, i.e., relatively large NH<sub>3</sub> VCDs were simulated  
617 | mostly in northern Jiangsu and northern Anhui province, consistent with the hotspot  
618 | of NH<sub>3</sub> emissions. The simulated NH<sub>3</sub> VCDs with E1 were 53% larger than those with  
619 | E2 across the whole YRD region, with the maximum and minimum monthly  
620 | difference calculated at 73% and 31% for April and October, respectively. The NMB,  
621 | NME, and correlation coefficient ( $r$ ) between [the](#) observed and simulated VCDs, and  
622 | the monthly average VCDs from observation and simulation are summarized in Table

带格式的: 字体: 倾斜

623 4. Application of both inventories resulted in larger NH<sub>3</sub> VCDs than those from  
624 | satellite observation for January and October, while the simulated VCDs for April and  
625 | July were smaller. Besides the uncertainty from monthly distribution of NH<sub>3</sub>  
626 | emissions, the bias from WRF modeling on temperature might also contribute to the  
627 | discrepancy between simulated and observed VCDs. As shown in Table S7 in the  
628 | supplement, WRF overestimated the monthly temperature in January and October  
629 | with the NMBs calculated at 26.6% and 0.34%, and underestimated it in April and  
630 | July with the NMBs calculated at -1.62% and -2.51%, respectively. Compared to E1,  
631 | application of E2 significantly reduced the NMEs from 83.8% to 37.5% for January  
632 | and largely corrected the overestimation in VCD simulation for January and October.  
633 | The simulated VCDs were 4.3% larger and 1.4% smaller than observation for the two  
634 | months, respectively. The results implied satisfying agreement between the simulated  
635 | and observed VCDs over the YRD region. Improvement in NH<sub>3</sub> VCD simulation was  
636 | also found for April when E2 instead of E1 was applied in the air quality modeling,  
637 | with the NME reduced from 65.8% to 60.7%. For July, however, application of E2 did  
638 | not improve the model performance, implying that current method in E2 could  
639 | possibly underestimate the NH<sub>3</sub> volatilization when the actual ambient temperature  
640 | was high. Besides the emissions, the discrepancy could result from various factors  
641 | including the uncertainty in chemical mechanisms in CMAQ and environmental  
642 | condition. Errors from satellite retrieval could also contribute to the inconsistency  
643 | between simulation and observation. van Damme et al. (2014), for example, estimated  
644 | an error of 19% for the total NH<sub>3</sub> columns in Asia. As the ESPRI product of NH<sub>3</sub>  
645 | VCDs we applied in the study does not provide the averaging kernel, moreover,  
646 | uncertainty in NH<sub>3</sub> column retrieval could result from the reduced sensitivity of  
647 | satellite measurement towards the surface.

删除的内容: s

删除的内容: IASI

带格式的: 下标

648 To further investigate the impact of soil pH on the emissions and thereby the  
649 | modeling performance on NH<sub>3</sub> VCDs, the soil in the YRD region was classified to  
650 | three types, acidic soil (pH≤6.5), neutral soil (6.5<pH≤7.5), and alkali soil (pH>7.5),  
651 | and the NMB<sub>s</sub> and NME<sub>s</sub> between the simulated and observed NH<sub>3</sub> VCDs were  
652 | calculated by soil type and month, as summarized in Table 5. For neutral and acidic  
653 | soil, application of E2 that considers the effect of farming season, geophysical  
654 | condition and manure management on NH<sub>3</sub> emission rates resulted in clearly smaller  
655 | NMEs than E1, implying the improvement in emission estimation. For acidic soil,  
656 | however, the NMBs were negative for all the months when E2 was applied, and the

659 NMEs were elevated compared to E1 except for January. Moreover, application of E2  
660 resulted in negative NMBs for neutral and alkali soil in April and July as well. Those  
661 results implied that E2 possibly underestimated the NH<sub>3</sub> emissions for acidic soil  
662 particularly for warm seasons. With the correction of pH and temperature, the NH<sub>3</sub>  
663 volatilization rate from basal dressing fertilization was relatively low, indicating that  
664 the current linear assumption between the soil pH and NH<sub>3</sub> volatilization rate might  
665 not be appropriate for soil with low pH values for eastern China. As shown in Figure  
666 S4 in the supplement, the measured NH<sub>3</sub> volatilization rates from urea and ABC  
667 fertilizer use under relatively high soil pH (Zhang et al., 2002; Zhong et al., 2006)  
668 were close to the estimated values in E2, but the measured results for acidic soil were  
669 clearly larger than those in E2.

删除的内容: near-

670 Limitation should be acknowledged in the emission comparison and evaluation.  
671 Besides those we paid extra attention to in E2 (e.g., temperature, soil property,  
672 fertilizer application method and manure management process), other factors could  
673 also be influential on air-surface exchange of NH<sub>3</sub> and thereby NH<sub>3</sub> emissions,  
674 including meteorology parameters (wind speed, precipitation, and leaf surface  
675 wetness), surface layer turbulence, air and surface heterogeneous-phase chemistry,  
676 and plant physiological conditions (Flechard et al. 2013; Gyldenkaerne et al., 2005,  
677 Skjoeth et al., 2011). With those factors integrated in a bi-directional  
678 surface-atmosphere exchange module in air quality modeling, the NH<sub>3</sub> emission  
679 inventories were improved and the biases in simulation of NH<sub>3</sub> and NH<sub>4</sub><sup>+</sup> aerosol  
680 concentrations were reduced for both US and Europe (Bash et al, 2013; Wichink Kruit  
681 et al., 2012). The ignorance of given parameters/process in current work could thus  
682 partly explain the discrepancy between the simulation and observation. Applying the  
683 bi-directional NH<sub>3</sub> exchange module, for example, Wichink Kruit et al. (2012) found  
684 increased NH<sub>3</sub> concentrations for agricultural source areas due to the elevated life  
685 time and transport distance of NH<sub>3</sub> in the model. The result implied a possible  
686 correction on the underestimation in NH<sub>3</sub> concentrations, as shown in Tables 3 and 4.  
687 Therefore, a more comprehensive evaluation and comparison in NH<sub>3</sub> emissions was  
688 thus suggested in the future, including the bi-directional NH<sub>3</sub> exchange and the  
689 top-down constraint with inversed modeling.

带格式的: 下标

带格式的: 下标

带格式的: 字体: Times New Roman, 非倾斜

带格式的: 下标

带格式的: 下标

带格式的: 下标

带格式的: 上标

带格式的: 下标

带格式的: 下标

带格式的: 下标

带格式的: 下标

带格式的: 下标

带格式的: 下标

### 690 3.4 Impacts of SO<sub>2</sub> and NO<sub>x</sub> emission estimates on simulated NH<sub>3</sub> and aerosols

692 Besides the meteorology condition, NH<sub>3</sub> emissions, and soil pH, the estimates of  
693 SO<sub>2</sub> and NO<sub>x</sub> emissions could influence the NH<sub>3</sub> and SIA simulation as well. SO<sub>2</sub> can  
694 be transformed to S (IV) through liquid phase reaction and then be oxidized to S (VI)  
695 by O<sub>3</sub>, or can be directly oxidized to H<sub>2</sub>SO<sub>4</sub> by H<sub>2</sub>O<sub>2</sub> or hydroxyl radical (•OH).  
696 HNO<sub>3</sub> can be formed through NO<sub>2</sub> oxidation by •OH at daytime, or through hydrolysis  
697 of N<sub>2</sub>O<sub>5</sub> at aerosol surface at night. Normally NH<sub>3</sub> preferentially reacts with H<sub>2</sub>SO<sub>4</sub>  
698 and relatively stable (NH<sub>4</sub>)<sub>2</sub>SO<sub>4</sub> is produced, while NH<sub>4</sub>NO<sub>3</sub> could easily be  
699 decomposed under high temperature or low humidity condition. Therefore, the  
700 ambient NH<sub>3</sub> concentrations and formation of NH<sub>4</sub><sup>+</sup> aerosols are influenced by the  
701 balance between acidic (SO<sub>2</sub> and NO<sub>x</sub>) and alkaline component (NH<sub>3</sub>) emissions.

702 As described in Section 2.3, the SO<sub>2</sub> and NO<sub>x</sub> emissions for 2014 used in this  
703 work were scaled from those for 2014 based on the changes in activity data. Ignorance  
704 of emission control progress during 2012-2014 would probably result in  
705 overestimation in emissions. The bias was evaluated through satellite observation. The  
706 daily planetary boundary layer (PBL) SO<sub>2</sub> and tropospheric NO<sub>2</sub> VCDs were obtained  
707 from the OMSO2 Level-3 product  
708 ([http://disc.sci.gsfc.nasa.gov/Aura/data-holdings/OMI/omso2e\\_v003.shtml](http://disc.sci.gsfc.nasa.gov/Aura/data-holdings/OMI/omso2e_v003.shtml)) and the  
709 POMINO Level-3 product from Ozone Monitoring Instrument (OMI), respectively.  
710 As shown in Table S8 in the supplement, all the provinces in YRD had their SO<sub>2</sub> and  
711 NO<sub>2</sub> VCDs substantially reduced during 2012-2014, and the VCDs declined by 48%  
712 and 31% respectively for the whole region. From a recent unpublished emission study,  
713 however, the SO<sub>2</sub> and NO<sub>x</sub> emissions were estimated to reduce only 16% and 8% in  
714 the YRD region for the two years (personal communication with Cheng Huang from  
715 Shanghai Research Academy of Environmental Science). It can be inferred that, the  
716 overestimation of SO<sub>2</sub> emissions might enhance their reaction with NH<sub>3</sub> and thereby  
717 the formation of (NH<sub>4</sub>)<sub>2</sub>SO<sub>4</sub> in the air quality modeling. The formation of NO<sub>3</sub><sup>-</sup>, in  
718 contrast, might be suppressed accordingly.

### 719 3.4.1 Identification of NH<sub>3</sub>-rich/-poor condition in YRD region

720 To evaluate the non-linear relation between gaseous pollutant emissions (SO<sub>2</sub>,  
721 NO<sub>x</sub> and NH<sub>3</sub>) and SIA concentrations for the YRD region, we follow Ansari and  
722 Pandis (1998) and calculated the gas ratio (GR) based on the modeling results:

$$723 \quad GR = \frac{([NH_3] + [NH_4^+]) - 2 \times [SO_4^{2-}]}{[NO_3^-] + [HNO_3]} \quad (7)$$

724 where the species in the bracket indicated the simulated ambient concentration. A  
725 negative GR indicates a NH<sub>3</sub>-poor condition, and the enhanced NH<sub>3</sub> emissions  
726 strengthen the oxidation of SO<sub>2</sub> and lead to increased SO<sub>4</sub><sup>2-</sup> (Wang et al., 2011). A GR  
727 larger than 1 indicates an NH<sub>3</sub>-rich condition. Enhanced NH<sub>3</sub> emissions have smaller  
728 effects on growth of SO<sub>4</sub><sup>2-</sup> concentrations, and elevated SO<sub>2</sub> emissions may accelerate  
729 the formation of NO<sub>3</sub><sup>-</sup> aerosols, as the increased NH<sub>4</sub><sup>+</sup> and SO<sub>4</sub><sup>2-</sup> reduce the NH<sub>4</sub>NO<sub>3</sub>  
730 capacity in the liquid phase (Seinfeld and Pandis, 2006). A neutral condition is judged  
731 when GR is between 0 and 1.

删除的内容: smaller than 0

732 Figure 10 illustrates the spatial distribution of simulated GR for the YRD region  
733 by month with E1 and E2 NH<sub>3</sub> inventories. Implied by the GR values larger than 1.0  
734 for most of the areas, the YRD region was identified under the NH<sub>3</sub>-rich condition  
735 when E1 was applied, except southwest Zhejiang. The judgment is consistent with  
736 previous studies (Wang et al., 2011; Dong et al., 2014). With the reduced NH<sub>3</sub>  
737 emissions in E2, the areas under neutral or NH<sub>3</sub>-poor condition expanded particularly  
738 for January and April. The common NH<sub>3</sub>-rich condition suggested potentially high  
739 sensitivity of SIA formation to SO<sub>2</sub> and NO<sub>x</sub> emissions.

删除的内容: The

#### 740 3.4.2 Sensitivities of NH<sub>3</sub> and SIA to SO<sub>2</sub> and NO<sub>x</sub> changes

741 Three more cases were developed to test the effect of SO<sub>2</sub> and NO<sub>x</sub> emission  
742 estimates on NH<sub>3</sub> and SIA simulation: Cases 1, 2 and 3 assumed 40% abatement of  
743 SO<sub>2</sub> emissions, 40% abatement of NO<sub>x</sub> emissions, and 40% abatement of emissions  
744 both species, respectively. E1 was applied for NH<sub>3</sub> emission estimates in all the cases.  
745 Table 6 summarizes the modeling performance at JSPAES and SHPD for different  
746 cases in October. Clear changes in NH<sub>3</sub> and SIA simulation were found with varied  
747 SO<sub>2</sub> emissions, while the effect of varied NO<sub>x</sub> emissions on air quality modeling was  
748 much smaller. The bias between the simulation and observation was partly corrected  
749 for most cases, indicated by the smaller NMBs. Indicated by NMEs, however, the  
750 modeling performance was less conclusive. NMEs for NH<sub>4</sub><sup>+</sup> and SO<sub>4</sub><sup>2-</sup> were reduced  
751 for Cases 1 and 3, while increased NMEs were found for NH<sub>3</sub> and NO<sub>3</sub><sup>-</sup>. Limitation in  
752 the mechanisms of SIA formation can be an important reason for the discrepancy.  
753 Under NH<sub>3</sub>-rich condition, abatement of SO<sub>2</sub> emissions (Case 1) would reduce the  
754 formation of (NH<sub>4</sub>)<sub>2</sub>SO<sub>4</sub>, and thereby lead to growth of NH<sub>3</sub> concentrations. This is  
755 consistent with the situation in North China Plain, another typical region suffering  
756 aerosol pollution in China (Liu et al., 2018). The simulated NH<sub>3</sub> were 10.1% and

删除的内容: secondary aerosol

760 11.7% larger than those in base case at JSPAES and SHPD, and the simulated SIA  
761 ( $\text{NH}_4^+ + \text{SO}_4^{2-} + \text{NO}_3^-$ ) were 7.9% and 11.0% smaller than those in base case at JSPAES  
762 and SHPD, respectively. Based on the modeling results in Table 3, as a comparison,  
763 the simulated  $\text{NH}_3$  concentrations with  $\text{NH}_3$  emissions in E2 were calculated 23% and  
764 28% smaller than those with E1 at JSPAES and SHPD for October, respectively, and  
765 the analogue number for SIA concentrations were 5% at both sites. While the  
766 estimation of  $\text{NH}_3$  emissions played an important role on  $\text{NH}_3$  simulation, the  $\text{SO}_2$   
767 estimation could be more effective on SIA simulation. Abatement of  $\text{NO}_x$  emissions  
768 (Case 2) was much less influential. Less  $\text{NO}_x$  slightly weakened the competition of  
769 SIA formation against  $\text{SO}_2$ , thus enhanced formation of  $(\text{NH}_4)_2\text{SO}_4$  and decreased  
770  $\text{NH}_3$  concentration were simulated at both sites, as shown in Table 6. When  $\text{SO}_2$  and  
771  $\text{NO}_x$  were simultaneously reduced in the model (Case 3), similar results were found  
772 with Case 1, implying again that  $\text{SO}_2$  could be a crucial species in SIA formation in  
773 the YRD region. In addition,  $\text{NO}_3^-$  aerosols were simulated to grow with the 40%  
774 abatement of  $\text{SO}_2$  and  $\text{NO}_x$  emissions, and the benefits of  $\text{SO}_2$  and  $\text{NO}_x$  control were  
775 partly weakened. To be more effective and efficient on regional air quality  
776 improvement, therefore, the control of  $\text{NH}_3$  emissions should be strengthened along  
777 with other pollutants.

778

779

#### 4. Conclusions

780 We took the YRD region in eastern China as an example and developed two  
781 inventories of  $\text{NH}_3$  emissions for 2014 based on the constant emission factors (E1)  
782 and those characterizing the agricultural processes (E2), respectively. Available  
783 information from ground and satellite observation was applied to evaluate the  
784 inventories through air quality modeling. Both inventories indicated that agricultural  
785 activities (livestock farming and fertilizer use) were the most important sources of  
786  $\text{NH}_3$ , but clear differences exist in estimates and spatial and seasonal distribution of  
787  $\text{NH}_3$  emissions. The total  $\text{NH}_3$  emissions in E1 were estimated 60% larger than E2,  
788 and the emissions from agriculture in E1 were double of E2. The information on  
789 fertilization season and type from local investigation in E2 resulted in discrepancies in  
790 monthly distributions of  $\text{NH}_3$  emissions from E1, particularly in northern YRD with  
791 abundant croplands. Differences in emission estimates lead to varied  $\text{NH}_3$   
792 concentrations from CMAQ modeling. At the suburban SHPD site, the overestimation

删除的内容: Yangtze River Delta areas

795 in NH<sub>3</sub> concentration from CMAQ with E1 could be largely corrected with E2,  
796 implying the improved estimation of NH<sub>3</sub> emissions by E2. At the urban site JSPAES,  
797 however, very limited improvement was achieved when E1 was replaced by E2 in the  
798 model, indicating that the emission estimation of local urban sources like  
799 transportation and residential activities were not improved in E2. Compared to NH<sub>3</sub>,  
800 the modeling performance for SIA is better for most cases, and differences between  
801 the simulated concentrations with E1 and E2 were clearly smaller. Application of E2  
802 improved the simulation of NH<sub>4</sub><sup>+</sup> and SO<sub>4</sub><sup>2-</sup> moderately. For the comparison with  
803 satellite-derived NH<sub>3</sub> column, application of E2 significantly corrected the  
804 overestimation in VCD simulation for January and October with E1, but did not  
805 improve the model performance for July. Combining the soil distribution, it can be  
806 inferred that current method might underestimate the NH<sub>3</sub> volatilization for acidic soil  
807 particularly in warm seasons. Judged by the simulated GR, most of the YRD region  
808 was identified as an NH<sub>3</sub>-rich condition except southwest Zhejiang. Through the  
809 sensitivity test in which SO<sub>2</sub> and NO<sub>x</sub> emissions were solely or simultaneously  
810 reduced, estimation of SO<sub>2</sub> emissions was detected to be more effective on SIA  
811 simulation compared to NH<sub>3</sub>. Reduced SO<sub>2</sub> emissions would suppress the formation  
812 of (NH<sub>4</sub>)<sub>2</sub>SO<sub>4</sub>, and thereby lead to growth of NH<sub>3</sub> concentrations. The control of NH<sub>3</sub>  
813 emissions should be strengthened along with that of SO<sub>2</sub> and NO<sub>x</sub> for improving the  
814 air quality more effectively and efficiently in the region.

删除的内容: inorganic aerosols

815 This work is a tentative effort on NH<sub>3</sub> emission evaluation at regional scale.  
816 The relations between environmental/meteorology conditions and NH<sub>3</sub> volatilization  
817 were not fully considered, and the bi-directional surface-atmosphere exchange was  
818 not included, resulting in bias in emission estimation. Uncertainties come also from  
819 the limitations in ground and satellite observation and incomplete mechanism of SIA  
820 formation in current air quality model. For better understanding the role of NH<sub>3</sub>  
821 emissions in regional air quality, more measurements on both sources and ambient  
822 concentrations are recommended in the future.

删除的内容: Given the insufficient field measurements, t

删除的内容:

删除的内容: (e.g., temperature and soil pH)

删除的内容: well

删除的内容: quantified

删除的内容: ,

删除的内容:

823

824

### Data availability

825 The Multi-resolution Emission Inventory for China used in this study was  
826 obtained at <http://www.meicmodel.org/> (last access: 31 July 2019, Tsinghua  
827 University, 2012). The high-resolution inventory for Jiangsu province was obtained in



838 Zhou et al. (2017) and can be accessed at <http://www.airqualitynju.com/> (last access:  
839 31 July 2019). The daily NH<sub>3</sub> VCDs measured through IASI was obtained from  
840 ESPRI data center at <http://cds-espri.ipsl.upmc.fr/etherTypo/index.php?id=1700&L=1>  
841 (last access: 31 July 2019). The two NH<sub>3</sub> emission inventories developed in this work  
842 (E1 and E2) will be available with the publication of this paper at  
843 <http://airquality.nju.com>.

844

845

#### **Author contributions**

846 YZ developed the strategy and methodology of the work and wrote the draft. MY  
847 ran the model and produced the figures. XH revised the method and provided useful  
848 comments. FC and JZ conducted ground observation of NH<sub>3</sub> and aerosols.

849

850

#### **Competing interests**

851 The authors declare that they have no conflict of interest.

852

853

#### **Acknowledgements**

854 This work was sponsored by Natural Science Foundation of China (91644220 and  
855 41575142) and the National Key Research and Development Program of China  
856 (2017YFC0210106). We would like to acknowledge Qizhen Liu and Zhong Zou from  
857 Shanghai Environmental Monitoring Center and Yunhua Chang from Nanjing  
858 University of Information Science & Technology for the ground measurement data,  
859 Qiang Zhang from Tsinghua University and Cheng Huang from Shanghai Research  
860 Academy of Environmental Science for emission data, and Simon Whitburn from  
861 Université Libre de Bruxelles and Yuanhong Zhao from Peking University for satellite  
862 data processing.

863

864

#### **References**

865 Ansari, A. S. and Pandis, S. N.: Response of inorganic PM to precursor concentrations.  
866 Environ. Sci. Technol., 32, 2706-2714, 1998.

867 [Bash, J. O., Cooter, E. J., Dennis, R. L., Walker, J. T., Pleim, J. E.: Evaluation of a](#)  
868 [regional air-quality model with bidirectional NH<sub>3</sub> exchange coupled to an](#)  
869 [agroecosystem model, Biogeosciences, 10, 1635-1645, 2013.](#)



870 Beusen, A. H. W., Bouwman, A. F., Heuberger, P. S. C., van Drecht, G., van der Hoek,  
871 K. W.: Bottom-up uncertainty estimates of global ammonia emissions from global  
872 agricultural production systems. *Atmos. Environ.*, 42, 6067-6077, 2008.

873 [Cai, G. X., Chen, D. L., Ding, H., Pacholski, A., Fan, X. H., Zhu, Z. L.: Nitrogen](#)  
874 [losses from fertilizers applied to maize, wheat and rice in the North China Plain. \*Nutr.\*](#)  
875 [\*Cycl. Agroecosys.\*, 63, 187-195, 2002.](#)

876 Chen, D., Zhao, Y., Lyu, R., Wu, R., Dai, L., Zhao, Y., Chen, F., Zhang, J., Yu, H.,  
877 Guan, M.: Seasonal and spatial variations of optical properties of light absorbing  
878 carbon and its influencing factors in a typical polluted city in Yangtze River Delta,  
879 China. *Atmos. Environ.*, 199, 45-54, 2019.

880 Chen, X., Walker, J. T., Geron, C.: Chromatography related performance of  
881 theMonitor for AeRosols and GAses in ambient air (MARGA): laboratory and  
882 field-based evaluation, *Atmos. Meas. Tech*, 10, 3893-3908, 2017.

883 Cheng, Y., Zheng, G., Wei, C., Mu, Q., Zheng, B., Wang, Z., Gao, M., Zhang, Q., He,  
884 K., Carmichael, G., Poschl, U., Su, H.: Reactive nitrogen chemistry in aerosol water as  
885 a source of sulfate during haze events in China, *Sci. Adv.*, 2, e1601530, doi:  
886 10.1126/sciadv.1601530, 2016.

887 Cheng, Z., Wang, S.X., Fu, X., Watson, J.G., Jiang, J., Fu, Q., Chen, C., Xu, B., Yu, J.,  
888 Chow, J.C., and Hao, J.: Impact of biomass burning on haze pollution in the Yangtze  
889 River delta, China: a case study in summer 2011, *Atmos. Chem. Phys.*, 14, 4573-4585,  
890 2014.

891 [Davies, D. K., Ilavajhala, S., Wong, M. M., and Justice, C. O.: Fire Information for](#)  
892 [Resource Management System: Archiving and Distributing MODIS Active Fire Data,](#)  
893 [IEEE Geosci. Remote Sens., 47, 72-79, 2009.](#)

894 Dong, W., Xin, J., Wang, S.: Temporal and spatial distribution of anthropogenic  
895 ammonia emissions in China: 1994–2006, *Environ. Sci.*, 31, 1457–1463, 2010 (in  
896 Chinese).

897 Dong, X., Li, J., Fu, J. S., Gao, Y., Huang, K., Zhuang, G.: Inorganic aerosols  
898 responses to emission changes in Yangtze River Delta, China. *Sci. Total Environ.*, 481,  
899 522-532, 2014.

900 [Emery, C., Tai, E., Yarwood, G.: Enhanced meteorological modeling and](#)  
901 [performance evaluation for two Texas episodes, Report to the Texas Natural](#)  
902 [Resources Conservation Commission, prepared by ENVIRON, International Corp,](#)  
903 [Novato, CA, 2001.](#)

904 European Environment Agency (EEA): EMEP/CORINAIR [Air Pollutant Emission](#)  
905 [Inventory Guidebook-2013, 3.B Manure management,](#) available at:  
906 <https://www.eea.europa.eu/publications/emep-eea-guidebook-2013/part-b-sectoral-guidance-chapters/4-agriculture/3-b-manure-management/view>, (last access: [25 Feb](#)  
907 [2020](#)), 2013a.

909 [European Environment Agency \(EEA\): EMEP/CORINAIR Air Pollutant Emission](#)  
910 [Inventory Guidebook-2013, 3.D Crop production and agricultural soils, available at:](#)  
911 <https://www.eea.europa.eu/publications/emep-eea-guidebook-2013/part-b-sectoral-guidance-chapters/4-agriculture/3-d-crop-production/view> (last access: [25 Feb 2020](#)),  
912 [2013b.](#)

914 [European Environment Agency \(EEA\): EMEP/CORINAIR Air Pollutant Emission](#)

删除的内容: Guo, H., Cheng, T., Gu, X., Wang, Y., Chen, H., Bao, F., Shi, S. Y., Xu, B. R., Wang, W. N., Zuo, X., Zhang, X. C., Meng, C.: Assessment of pm<sub>2.5</sub> concentrations and exposure throughout china using ground observations, *Sci. Total Environ.*, 1024, 601-602, 2017. .

删除的内容: <http://www.eea.europa.eu/publications/emep-eea-guidebook-2013>

删除的内容: 9

删除的内容: March 2019

928 [Inventory Guidebook-2009, 4.D Crop production and agricultural soils, available at:](https://www.eea.europa.eu/publications/emep-eea-emission-inventory-guidebook-2009/part-b-sectoral-guidance-chapters/4-agriculture/4-d/4-d-crop-production-and-agricultural-soils.pdf/view)  
929 [https://www.eea.europa.eu/publications/emep-eea-emission-inventory-guidebook-200](https://www.eea.europa.eu/publications/emep-eea-emission-inventory-guidebook-2009/part-b-sectoral-guidance-chapters/4-agriculture/4-d/4-d-crop-production-and-agricultural-soils.pdf/view)  
930 [9/part-b-sectoral-guidance-chapters/4-agriculture/4-d/4-d-crop-production-and-agricul](https://www.eea.europa.eu/publications/emep-eea-emission-inventory-guidebook-2009/part-b-sectoral-guidance-chapters/4-agriculture/4-d/4-d-crop-production-and-agricultural-soils.pdf/view)  
931 [tural-soils.pdf/view](https://www.eea.europa.eu/publications/emep-eea-emission-inventory-guidebook-2009/part-b-sectoral-guidance-chapters/4-agriculture/4-d/4-d-crop-production-and-agricultural-soils.pdf/view) (last access: 25 Feb 2020), 2009.

932 Fang, X., Shen, G., Xu, C., Qian, X., Li, J., Zhao, Z., Yu, S., Zhu, K.: Agricultural  
933 ammonia emission inventory and its distribution characteristics in Shanghai, *Acta*  
934 *Agriculturae Zhejiangensis*, 27, 2177-2185, 2015 (in Chinese).

935 [Flechar, C. R., Massad, R.-S., Loubet, B., Personne, E., Simpson, D., Bash, J. O.,](#)  
936 [Cooter, E. J., Nemitz, E., Sutton, M. A.: Advances in understanding, models and](#)  
937 [parameterizations of biosphere-atmosphere ammonia exchange, \*Biogeosciences\*, 10,](#)  
938 [5183-5225, 2013.](#)

939 Fu, X., Wang, S., Xing, J., Zhang, X., Wang, T., Hao, J.: Increasing ammonia  
940 concentrations reduce the effectiveness of particle pollution control achieved via SO<sub>2</sub>  
941 and NO<sub>x</sub> emissions reduction in east China. *Environ. Sci. Technol. Lett.*, 4, 221-227,  
942 2017

943 Fu, X., Wang, S., Ran, L., Pleim, J. E., Cooter, E., Bash, J. O., Benson, V., Hao, J.:  
944 Estimating NH<sub>3</sub> emissions from agricultural fertilizer application in China using the  
945 bi-directional CMAQ model coupled to an agro-ecosystem model. *Atmos. Chem.*  
946 *Phys.*, 15, 6637-6649, 2015.

947 [Guenther, A. B., Jiang, X., Heald, C. L., Sakulyanontvittaya, T., Duhl, T., Emmons, L.,](#)  
948 [K., Wang, X.: The Model of Emissions of Gases and Aerosols from Nature version 2.1](#)  
949 [\(MEGAN2.1\): an extended and updated framework for modeling biogenic emissions.](#)  
950 [\*Geosci. Model Dev.\*, 5, 1471-1492, 2012.](#)

951 [Guo, H., Cheng, T., Gu, X., Wang, Y., Chen, H., Bao, F., Shi, S. Y., Xu, B. R., Wang,](#)  
952 [W. N., Zuo, X., Zhang, X. C., Meng, C.: Assessment of PM<sub>2.5</sub> concentrations and](#)  
953 [exposure throughout China using ground observations, \*Sci. Total Environ.\*, 1024,](#)  
954 [601-602, 2017.](#)

955 [Gyldenkaerne, S., Skjøth, C., Hertel, O., Ellermann, T. A.: Dynamical ammonia](#)  
956 [emission parameterization for use in air pollution models, \*J. Geophys. Res.\*, 110,](#)  
957 [D07108, doi:10.1029/2004JD005459, 2005.](#)

958 [Huo, Q., Cai, X., Kang, L., Zhang, H., Song, Y., Zhu, T.: Estimating ammonia](#)  
959 [emissions from a winter wheat cropland in North China Plain with field experiments](#)  
960 [and inverse dispersion modeling, \*Atmos. Environ.\*, 104, 1-10, 2015.](#)

961 Huang, R., Zhang, Y., Bozzetti, C., Ho, K., Cao, J., Han, Y., Daellenbach, K. R.,  
962 Slowik, J. G., Platt, S. M., Canonaco, F., Zotter, P., Wolf, R., Pieber, S. M., Bruns, E.  
963 A., Crippa, M., Ciarelli, G., Piazzalunga, A., Schwikowski, M., Abbaszade, G.,  
964 Schnelle-Kreis, J., Zimmermann, R., An, Z., Szidat, S., Baltensperger, U., El Haddad,  
965 I., Prevot, A. S. H.: High secondary aerosol contribution to particulate pollution  
966 during haze events in China, *Nature*, 514, 218-222, 2014.

967 Huang, X., Song, Y., Li, M., Li, J., Huo, Q., Cai, X., Zhu, T., Hu, M., Zhang, H.: A  
968 high-resolution ammonia emission inventory in China. *Global Biogeochem. Cy.*, 26,  
969 GB1030, doi: 10.1029/2011GB004161, 2012.

970 [Kang, Y., Liu, M., Song, Y., Huang, X., Yao, H., Cai, X., Zhang, H., Kang, L., Liu, X.,](#)  
971 [Yan, X., He, H., Zhang, Q., Shao, M., Zhu, T.: High-resolution ammonia emissions](#)  
972 [inventories in China from 1980 to 2012, \*Atmos. Chem. Phys.\*, 16, 2043-2058, 2016.](#)

删除的内容: .

带格式的: 字体: Times New Roman

带格式的: 无孤行控制, 调整中文与西文文字的间距, 调整中文与数字的间距

带格式的: 字体: Times New Roman

带格式的: 字体: Times New Roman

带格式的: 字体: Times New Roman

带格式的: 字体: Times New Roman

带格式的: 字体: Times New Roman

删除的内容: Li, B., Zhang, J., Zhao, Y., Yuan, S., Zhao, Q., Shen, G., Wu, H.: Seasonal variation of urban carbonaceous aerosols in a typical city Nanjing in Yangtze River Delta, China. *Atmos. Environ.*, 106, 223-231, 2015. . Liu, X., Zhang, Y., Han, W., Tang, A., Shen, J., Cui, Z., Vitousek, P., Erisman, J. W., Goulding, K., Christie, P., Fangmeier, A., Zhang, F.: Enhanced nitrogen deposition over China. *Nature*, 494, 459-463, 2013. .

删除的内容: Seinfeld, J. H. and Pandis, S. N.: From air pollution to climate change. *Atmos. Chem. Phys.*, 6, 429-443, 2006. .

990 Kurokawa, J., Ohara, T., Morikawa, T., Hanayama, S., Janssens-Maenhout, G., Fukui,  
991 T., Kawashima, K., and Akimoto, H.: Emissions of air pollutants and greenhouse  
992 gases over Asian regions during 2000-2008: Regional Emission inventory in ASia  
993 (REAS) version 2, *Atmos. Chem. Phys.*, 13, 11019-11058, 2013.

994 Lanciki, A.: 2060 MARGA Monitor for AeRosols and Gases in ambient Air. Metrohm  
995 Process Analytics, Switzerland, available at:  
996 <https://www.metrohm.com/en/products/process-analyzers/applikon-marga/> (last  
997 access: 10 Feb, 2020), 2018.

998 Li, B., Zhang, J., Zhao, Y., Yuan, S., Zhao, Q., Shen, G., Wu, H.: Seasonal variation of  
999 urban carbonaceous aerosols in a typical city Nanjing in Yangtze River Delta, China.  
1000 *Atmos. Environ.*, 106, 223-231, 2015.

1001 Li, L.: The numerical simulation of comprehensive air pollution characteristics in a  
1002 typical city-cluster, Ph. D thesis, Shanghai University, Shanghai, China, 2012.

1003 Liu, C., Yao, L.: Agricultural ammonia emission inventory and its distribution  
1004 characteristics in Jiangsu Province, *Journal of Anhui Agri. Sci.*, 44, 70-74, 2016 (in  
1005 Chinese).

1006 Liu, M., Huang, X., Song, Y., Xu, T., Wang, S., Wu, Z., Hu, M., Zhang, L., Zhang, Q.,  
1007 Pan, Y., Liu, X., Zhu, T.: Rapid SO<sub>2</sub> emission reductions significantly increase  
1008 tropospheric ammonia concentrations over the North China Plain, *Atmos. Chem. Phys.*,  
1009 18, 17933-17943, 2018

1010 Liu, X., Zhang, Y., Han, W., Tang, A., Shen, J., Cui, Z., Vitousek, P., Erisman, J. W.,  
1011 Goulding, K., Christie, P., Fangmeier, A., Zhang, F.: Enhanced nitrogen deposition  
1012 over China. *Nature*, 494, 459-463, 2013.

1013 Ministry of Environmental Protection (MEP), The Guideline of Emission Inventory  
1014 Development for Atmospheric Ammonia, 2014 (in Chinese)

1015 National Development and Reform Commission of China (NDRC): National data on  
1016 the cost and profit of agricultural product, China Statistics Press, Beijing, 2015 (in  
1017 Chinese).

1018 Pan, Y., Tian, S., Zhao, Y., Zhang, L., Zhu, X., Gao, J., Huang, W., Zhou, Y., Song, Y.,  
1019 Zhang, Q., Wang, Y.: Identifying ammonia hotspots in China using a national  
1020 observation network. *Environ. Sci. Technol.*, 52, 3926-3934, 2018.

1021 Pan, Y., Wang, Y., Tang, G., Wu, D.: Wet and dry deposition of atmospheric nitrogen  
1022 at ten sites in Northern China, *Atmos. Chem. Phys.*, 12, 6515-6535, 2012.

1023 Paulot, F., Fan, S., Horowitz, L. W.: Contrasting seasonal responses of sulfate aerosols  
1024 to declining SO<sub>2</sub> emissions in the Eastern US: implications for the efficacy of SO<sub>2</sub>  
1025 emission controls, *Geophys. Res. Lett.*, 44, 455-464, doi: 10.1002/2016GL070695,  
1026 2017.

1027 Price, C., Penner, J., Prather, M.: NO<sub>x</sub> from lightning, Part I: Global distribution  
1028 based on lightning physics, *J. Geophys. Res.-Atmos.*, 102, 5929-5941, doi:  
1029 10.1029/96JD03504, 1997.

1030 Qin, M., Wang, X., Hu, Y., Huang, X., He, L., Zhong, L., Song, Y., Hu, M. and Zhang,  
1031 Y.: Formation of particulate sulfate and nitrate over the Pearl River Delta in the fall:  
1032 Diagnostic analysis using the Community Multiscale Air Quality model. *Atmos.*  
1033 *Environ.*, 112, 81-89, 2015.

删除的内容: 2

删除的内容: Nov

删除的内容: .

删除的内容: 2019

删除的内容: Li, L.: The numerical simulation of comprehensive air pollution characteristics in a typical city-cluster, Ph. D thesis, Shanghai University, Shanghai, China, 2012. .

删除的内容: .

1044 [Schaap, M., Otjes, R. P., Weijers, E. P.: Illustrating the benefit of using hourly](#)  
1045 [monitoring data on secondary inorganic aerosol and its precursors for model](#)  
1046 [evaluation. Atmos. Chem. Phys., 11, 11041–11053, 2011](#)

1047 Seinfeld, J. H. and Pandis, S. N.: From air pollution to climate change. Atmos. Chem.  
1048 Phys., 6, 429-443, 2006.

1049 Sindelarova, K., Granier, C., Bouarar, I., Guenther, A., Tilmes, S., Stavrou, T.,  
1050 Müller, J.-F., Kuhn, U., Stefani, P., and Knorr, W.: Global data set of biogenic VOC  
1051 emissions calculated by the MEGAN model over the last 30 years, Atmos. Chem.  
1052 Phys., 14, 9317–9341, 2014.

1053 [Skamarock, W. C., Klemp, J. B., Dudhia, J., Gill, D. O., Barker, D. M., Duda, M. G.,](#)  
1054 [Huang, X.-Y., Wang, W., Powers, J. G. A Description of the Advanced Research WRF](#)  
1055 [Version 3. NCAR Tech. Note NCAR/TN-475+STR, 113 pp.doi:10.5065/D68S4MVH,](#)  
1056 [2008.](#)

1057 [Skjoeth, C. A., Geels, C., Berge, H., Gyldenkaerne, S., Fagerli, H., Ellermann, T.,](#)  
1058 [Frohn, L. M., Christensen, J., Hansen, K. M., Hansen, K., Hertel, O.: Spatial and](#)  
1059 [temporal variations in ammonia emissions - a freely accessible model code for Europe,](#)  
1060 [Atmos. Chem. Physics, 11, 5221-5236, 2011.](#)

1061 [Stieger, B., Spindler, G., Fahlbusch, B. Muller, K., Gruner, A., Poulain, L., Thoni, L.,](#)  
1062 [Seitler, E., Wallasch, M., Herrmann, H.: Measurements of PM<sub>10</sub> ions and trace gases](#)  
1063 [with the online system MARGA at the research station Melpitz in Germany - A](#)  
1064 [five-year study. J. Atmos. Chem., 75, 33-70, 2018.](#)

1065 [Su, F., Huang, B., Ding, X., Gao, Z., Chen, X., Zhang, F., Kogge, M., Römheld, V.:](#)  
1066 [Ammonia volatilization of different nitrogen fertilizer types, Soils, 38, 682-686, 2006](#)  
1067 [\(in Chinese\).](#)

1068 [Sutton, M. A., Dragosits, U., Tang, Y. S., Fowler, D.; Ammonia emissions from](#)  
1069 [nonagricultural sources in the UK. Atmos. Environ., 34, 855-869, 2000,](#)

1070 [Sutton, M., Place, C., Eager, M., Fowler, D., Smith, R.; Assessment of the magnitude](#)  
1071 [of ammonia emissions in the United-Kingdom, Atmos. Environ., 29, 1393-1411,](#)  
1072 [1995.](#)

1073 [University of North Carolina at Chapel Hill \(UNC\): Operational Guidance for the](#)  
1074 [Community Multiscale Air Quality \(CMAQ\) Modeling System Version 4.7.1 \(June](#)  
1075 [2010 Release\), available at http://www.cmaq-model.org \(last access: 10 Feb 2020\),](#)  
1076 [2010.](#)

1077 U.S. Environmental Protection Agency (USEPA): Compilation of Air Pollutant  
1078 Emission Factors, available at <http://www.epa.gov/ttn/chief/ap42/index.html> (last  
1079 access: 9 March 2019), 2002.

1080 van Damme, M., Clarisse, L., Dammers, E., Liu, X., Nowak, J. B., Clerbaux, C.,  
1081 Flechard, C. R., Galyalcaux, C., Xu, W., Neuman, J. A.: Towards validation of  
1082 ammonia (NH<sub>3</sub>) measurements from the IASI satellite, Atmos. Meas. Tech., 8,  
1083 1575-1591, 2015

1084 van Damme, M., Clarisse, L., Heald, C. L., Hurtmans, D., Ngadi, Y., Clerbaux, C.,  
1085 Dolman, A. J., Erisman, J. W., Coheur, P. F.: Global distributions, time series and error  
1086 characterization of atmospheric ammonia (NH<sub>3</sub>) from IASI satellite observations.  
1087 Atmos. Chem. Phys., 14, 2905-2922, 2014.

带格式的：下标

带格式的：字体：（默认）Times  
New Roman，小四

带格式的：字体：（默认）Times  
New Roman，小四

带格式的：字体：（默认）Times  
New Roman，小四

带格式的：两端对齐，定义网格后  
自动调整右缩进，段落间距段前：  
0.5 行，段后：0.5 行，孤行控制

带格式的：字体：（默认）Times  
New Roman，小四

带格式的：字体：（默认）Times  
New Roman，小四

带格式的：字体：（默认）Times  
New Roman，小四

带格式的：字体：（默认）Times  
New Roman，小四

带格式的：字体：（默认）Times  
New Roman，小四

带格式的：字体：（默认）Times  
New Roman，小四

带格式的：字体：（默认）Times  
New Roman，小四

1088 Warner, J. X., Dickerson, R. R., Wei, Z., Strow, L. L., Wang, Y., Liang, Q.: Increased  
1089 atmospheric ammonia over the world's major agricultural areas detected from space.  
1090 Geophys. Res. Lett, 44, 2875-2884, doi: 10.1002/2016GL072305, 2017.

1091 Wang, G., Zhang, R., Gomez, M. E., Yang, L., Zamora, M. L., Hu, M., Lin, Y., Peng,  
1092 J., Guo, S., Meng, J., Li, J., Cheng, C., Hu, T., Ren, Y., Wang, Y., Gao, J., Cao, J., An,  
1093 Z., Zhou, W., Li, G., Wang, J., Tian, P., Marrero-Ortiz, W., Secret, J., Du, Z., Zheng,  
1094 J., Shang, D., Zeng, L., Shao, M., Wang, W., Huang, Y., Wang, Y., Zhu, Y., Li, Y., Hu,  
1095 J., Pan, B., Cai, L., Cheng, Y., Ji, Y., Zhang, F., Rosenfeld, D., Liss, P. S., Duce, R. A.,  
1096 Kolb, C. E., Molina, M. J.: Persistent sulfate formation from London Fog to Chinese  
1097 haze, P Natl. Acad. SCI. USA, 113, 13630-13635, 2016.

1098 Wang, S., Xing, J., Jang, C., Zhu, Y., Fu, J. S., Hao, J.: Impact assessment of ammonia  
1099 emissions on inorganic aerosols in east China using response surface modeling  
1100 technique. Environ. Sci. Technol., 45, 9293-9300, 2011.

1101 Wei, L., Duan, J., Tan, J., Ma, Y., He, K., Wang, S., Huang, X., Zhang, Y.:  
1102 Gas-to-particle conversion of atmospheric ammonia and sampling artifacts of  
1103 ammonium in spring of Beijing. Science China, 45, 216-226, 2015 (in Chinese).

1104 [Wichink Kruit, R. J., Schaap, M., Sauter, F. J., van Zanten, M. C., van Pul, W. A. J.:  
1105 Modeling the distribution of ammonia across Europe including bi-directional surface  
1106 atmosphere exchange, Biogeosciences, 9, 5261-5277, 2012.](#)

1107 Xiao, Z. M., Zhang, Y. F., Hong, S. M., Bi, X. H., Jiao, L., Feng, Y. C., and Wang, Y.  
1108 Q.: Estimation of the main factors influencing haze, based on a long-term monitoring  
1109 Campaign in Hangzhou, China. Aerosol Air Qual. Res., 11, 873-882, 2011.

1110 Yang, F., Tan, J., Zhao, Q., Du, Z., He, K., Ma, Y., Duan, F., Chen, G., Zhao, Q.:  
1111 Characteristics of PM<sub>2.5</sub> speciation in representative megacities and across China,  
1112 Atmos. Chem. Phys. 11, 5207-5219, 2011.

1113 Yang, Y., Zhao, Y.: Quantification and evaluation of atmospheric pollutant emissions  
1114 from open biomass burning with multiple methods: A case study for Yangtze River  
1115 Delta region, China. Atmos. Chem. Phys. 19, 327-348, 2019.

1116 Yang, Z.: Estimation of ammonia emission from livestock in China based on  
1117 mass-flow method and regional comparison, Master thesis, Peking University, Beijing,  
1118 China, 2008.

1119 Yu, F., Chao, N., Wu, J., Tang, G., Chen, J., Wang, H., Wu, Z.: Research on  
1120 agricultural ammonia emission inventory of Zhejiang Province in 2013,  
1121 Environmental Pollution & Control, 38, 41-46, 2016 (in Chinese).

1122 Zhang, F, Chen, X., Chen, Q.: The fertilization guideline for the main crop types in  
1123 China, China Agricultural University Press, Beijing, 2009 (in Chinese).

1124 Zhang, L., Chen, Y., Zhao, Y., Henze, D. K., Zhu, L., Song, Y., Paulot, F., Liu, X., Pan,  
1125 Y., Lin, Y., Huang, B.: Agricultural ammonia emissions in China: reconciling  
1126 bottom-up and top-down estimates, Atmos. Chem. Phys., 18, 339-355, 2018.

1127 Zhang, Q., Zhang, M., Yang, Y., Lu, J.: Volatilization of ammonium bicarbonate and  
1128 urea in main soil of Shandong Province, Chinese Journal of Soil Science, 33, 32-34,  
1129 2002.

- 1130 Zhang, X., Wu, Y., Liu, X., Reis, S., Jin, J., Dragosits, U., van Damme, M., Clarisse,  
1131 L., Whitburn, S., Coheur, P. F., Gu, B.: Ammonia emissions may be substantially  
1132 underestimated in China. *Environ. Sci. Technol.*, 12089-12096, 2017.
- 1133 Zhang, X., Wang, Y., Niu, T., Zhang, X., Gong, S., Zhang, Y., Sun, J.: Atmospheric  
1134 aerosol compositions in China: spatial/temporal variability, chemical signature,  
1135 regional haze distribution and comparisons with global aerosols, *Atmos. Chem. Phys.*  
1136 *12*, 779-799, 2012.
- 1137 Zhang, Y., Bo, X., Zhao, Y., and Nielsen, C. P.: Benefits of current and future policies  
1138 on emissions of China's coal- fired power sector indicated by continuous emission  
1139 monitoring, *Environ. Pollut.*, submitted, 2019.
- 1140 [Zhang, Y., Dore, A. J., Ma, L., Liu, X., Ma, W., Cape, J. N., Zhang, F.: Agricultural](#)  
1141 [ammonia emissions inventory and spatial distribution in the North China Plain.](#)  
1142 [\*Environ. Pollut.\*, 158, 490-501, 2010.](#)
- 1143 Zhao, B., Wang, S., Wang, J, Fu, J. S., Liu, T, Xu, J, Fu, X., Hao, J: Impact of national  
1144 NO<sub>x</sub> and SO<sub>2</sub> control policies on particulate matter pollution in China, *Atmos.*  
1145 *Environ.*, 77, 453–463, 2013.
- 1146 Zhao, Y., Mao, P., Zhou, Y., Yang, Y., Zhang, J., Wang, S., Dong, Y., Xie, F., Yu, Y., Li,  
1147 W.: Improved provincial emission inventory and speciation profiles of anthropogenic  
1148 non-methane volatile organic compounds: a case study for Jiangsu, China, *Atmos.*  
1149 *Chem. Phys.*, 17, 7733-7756, 2017
- 1150 Zhao, Y., Qiu, L., Xu, R., Xie, F., Zhang, Q., Yu, Y., Nielsen, C. P., Qin, H., Wang, H.,  
1151 Wu, X., Li, W., Zhang, J.: Advantages of city-scale emission inventory for urban air  
1152 quality research and policy: the case of Nanjing, a typical industrial city in the  
1153 Yangtze River Delta, China, *Atmos. Chem. Phys.*, 15, 12623-12644, 2015.
- 1154 Zheng, H., Cai, S., Wang, S., Zhao, B., Chang, X., and Hao, J.: Development of a  
1155 unit-based industrial emission inventory in the Beijing–Tianjin–Hebei region and  
1156 resulting improvement in air quality modeling. *Atmos. Chem. Phys.*, 19, 3447–3462,  
1157 2019.
- 1158 Zheng, Z., Weng, J., Wang, S., Wang, J.: Estimation of ammonia emission in Anhui  
1159 Province, *Journal of Anhui Agricultural Sciences*, 8, 73-75, 2016 (in Chinese).
- 1160 Zhong, N., Zeng, Q., Zhang, L., Liao, B., Zhou, X., Jiang, J.: Effects of acidity and  
1161 alkalinity on urea transformation in soil, *Chinese Journal of Soil Science*, 37,  
1162 1123-1128, 2006 [\(in Chinese\)](#).
- 1163 Zhou, Y., Zhao, Y., Mao, P., Zhang, Q., Zhang, J., Qiu, L., Yang, Y.: Development of a  
1164 high-resolution emission inventory and its evaluation and application through air  
1165 quality modeling for Jiangsu Province, China, *Atmos. Chem. Phys.*, 17, 211–233,  
1166 2017.

带格式的: 非突出显示



## FIGURE CAPTIONS

Figure 1. **Research domain.** The blue dots and red triangles indicate the locations of 43 meteorological monitoring sites and 2 air quality monitoring sites, respectively, and the numbers of 1–41 represent the prefectural cities of Fuyang, Bozhou, Huaibei, Suzhou, Liuan, Hefei, Huainan, Bengbu, Chuzhou, Anqing, Tongling, Wuhu, Maanshan, Chizhou, Xuancheng, Huangshan, Xuzhou, Suqian, Lianyungang, Huaian, Yancheng, Yangzhou, Taizhou, Nanjing, Zhenjiang, Changzhou, Wuxi, Suzhou, Nantong, Huzhou, Jiaxing, Hangzhou, Shaoxing, Ningbo, Zhoushan, Quzhou, Jinhua, Taizhou, Lishui, Wenzhou, and Shanghai. The map data provided by Resource and Environment Data Cloud Platform are freely available for academic use (<http://www.resdc.cn/data.aspx?DATAID=201>).

删除的内容: Studying area and r

Figure 2. Differences of fertilizer application between the two inventories in YRD ( $RD = (E_1 - E_2)/(E_1 + E_2)/2$ ).

Figure 3. The spatial distribution of monthly average of  $\text{NH}_3$  vertical columns over YRD region from IASI satellite observation (Unit:  $10^{15}$  **molecule/cm<sup>2</sup>**).

删除的内容: mole.

Figure 4. Monthly  $\text{NH}_3$  emissions from fertilizer use and livestock farming in E1 and E2.

Figure 5. Spatial distribution of  $\text{NH}_3$  emissions from fertilizer use, livestock farming and all categories in E1 and E2.

Figure 6. Differences of  $\text{NH}_3$  emissions from fertilizer use and all categories between the two inventories ( $RD = (E_1 - E_2)/(E_1 + E_2)/2$ ).

Figure 7. Comparison between the estimated  $\text{NH}_3$  emissions in this work and other studies by province and source category. "Others" indicate Fang et al. (2015), Liu and Yao (2016), Yu et al. (2016), and Zheng et al. (2016) for Shanghai, Jiangsu, Zhejiang, and Anhui, respectively.

Figure 8. The observed and simulated hourly  $\text{NH}_3$  and SIA concentrations with the two inventories at JSPAES and SHPD sites

Figure 9. The  $\text{NH}_3$  VCDs in the YRD region simulated with the two inventories by month.

Figure 10. The GR values in the YRD region simulated with the two inventories by month.

## TABLES

**Table 1. Anthropogenic NH<sub>3</sub> emission source categories**

Category	Subcategory	Category	Subcategory
Fertilizer application	urea	Fuel combustion	industrial coal combustion
	ammonium bicarbonate		industrial oil combustion
	ammonium nitrate		industrial gas combustion
	ammonium sulfate		domestic coal combustion
	compound fertilizer		domestic oil combustion
Livestock Farming	beef cattle	Biomass burning	domestic gas combustion
	dairy cow		straw burning
	horse/donkey/mule		domestic firewood
	sow	Transportation	open
	hog		light duty gasoline vehicle
	goat		heavy duty gasoline vehicle
	sheep		light duty diesel vehicle
	layer		heavy duty diesel vehicle
	laying duck		motorcycle
	broiler	Sewage and waste treatment	waste landfill
	duck		waste incineration
	goose		waste compost
	rabbit		sewage treatment
Human being	cattle/buffalo	Industry sources	ammonium synthesis
	human sweat		nitrogenous fertilizer
	human breath		phosphate fertilizer
	human excretion		coking
	baby excretion		



**Table 2. Two anthropogenic NH<sub>3</sub> emission inventories in the YRD region in 2014 (Gg)**

	Method	Livestock	Fertilizer	Chemical Industry	Biomass Burning	Waste Disposal	Traffic	Fuel Combustion	Human Beings	Total
Shanghai	E <sub>1</sub>	14.9	11.9	0.1	0.3	5.0	1.9	5.1	5.5	44.5
	E <sub>2</sub>	6.5	9.0							33.2
Jiangsu	E <sub>1</sub>	340.8	357.4	14.1	29.1	6.0	8.6	5.2	30.8	791.9
	E <sub>2</sub>	145.6	257.1							496.5
Zhejiang	E <sub>1</sub>	115.7	93.8	2.4	10.6	6.9	7.7	4.7	28.3	270.1
	E <sub>2</sub>	37.4	49.3							147.2
Anhui	E <sub>1</sub>	241.5	314.9	14.7	35.9	2.8	3.3	7.3	37.7	658.2
	E <sub>2</sub>	102.3	185.9							389.9
Total	E <sub>1</sub>	712.7	778.0	31.2	75.9	20.7	21.6	22.3	102.2	1764.7
	E <sub>2</sub>	291.8	501.3							1067.0

**Table 3. Model performance statistics for the hourly concentrations of NH<sub>3</sub> and SIA from observation and CMAQ simulation with the two inventories at SHPD and JSPAES sites for available months.**

Indicator	SHPD_Apr		SHPD_July		SHPD_Oct		JSPAES_Oct		
	E <sub>1</sub>	E <sub>2</sub>	E <sub>1</sub>	E <sub>2</sub>	E <sub>1</sub>	E <sub>2</sub>	E <sub>1</sub>	E <sub>2</sub>	
NH <sub>3</sub>	NMB (%)	75.11	17.02	15.62	-12.85	32.32	-5.05	1.73	-21.75
	NME (%)	141.08	103.59	88.72	78.00	98.36	76.25	56.94	53.68
	r (p<0.01)	0.23	0.23	0.25	0.23	0.20	0.18	0.35	0.33
	Mean sim. (μg/m <sup>3</sup> )	7.12	4.76	10.70	8.06	7.39	5.30	7.75	5.96
	Mean obs. (μg/m <sup>3</sup> )	4.58		9.25		5.58		7.62	
NH <sub>4</sub> <sup>+</sup>	NMB (%)	-8.78	-19.14	12.98	6.11	84.45	74.02	15.01	9.53
	NME (%)	40.07	40.78	64.26	61.76	100.23	91.69	42.27	40.7
	r (p<0.01)	0.66	0.66	0.57	0.56	0.58	0.57	0.57	0.57
	Mean sim. (μg/m <sup>3</sup> )	6.91	6.13	7.04	6.61	7.64	7.21	10.97	10.45
	Mean obs. (μg/m <sup>3</sup> )	7.58		6.23		4.14		9.54	
SO <sub>4</sub> <sup>2-</sup>	NMB (%)	24.08	14.05	50.86	46.84	91.92	90.41	14.38	12.53
	NME (%)	57.59	51.61	84.63	81.15	110.18	108.61	43.65	42.31
	r (p<0.01)	0.55	0.54	0.46	0.47	0.42	0.44	0.34	0.36
	Mean sim. (μg/m <sup>3</sup> )	14.75	13.56	14.60	14.21	14.53	14.41	15.5	15.25
	Mean obs. (μg/m <sup>3</sup> )	11.89		9.68		7.57		13.56	
NO <sub>3</sub> <sup>-</sup>	NMB (%)	-59.13	-65.20	-78.10	-94.24	29.46	12.60	-6.55	-14.18
	NME (%)	65.72	70.16	141.43	142.86	93.69	70.54	44.81	44.94
	r (p<0.01)	0.49	0.50	0.51	0.52	0.53	0.49	0.62	0.61
	Mean sim. (μg/m <sup>3</sup> )	4.93	4.19	5.39	4.64	7.32	6.37	17.53	16.1
	Mean obs. (μg/m <sup>3</sup> )	12.05		9.01		5.65		18.76	

Note: obs. and sim. indicate the results from observation and simulation, respectively. The NMB and NME were calculated using following equations (P and O indicates the results from modeling prediction and observation, respectively):

$$NMB = \frac{\sum_{i=1}^n (P_i - O_i)}{\sum_{i=1}^n O_i} \times 100\% ; \quad NME = \frac{\sum_{i=1}^n |P_i - O_i|}{\sum_{i=1}^n O_i} \times 100\%$$

**Table 4. Model performance statistics for the daily NH<sub>3</sub> VCDs from IASI observation and CMAQ simulation using the two inventories by month.**

	January		April		July		October	
	E <sub>1</sub>	E <sub>2</sub>	E <sub>1</sub>	E <sub>2</sub>	E <sub>1</sub>	E <sub>2</sub>	E <sub>1</sub>	E <sub>2</sub>
NMB(%)	77.02	4.29	28.49	-59.12	12.19	-34.12	29.46	-1.77
NME(%)	83.83	37.54	65.8	60.07	43.93	51.91	46.38	43.17
r ( <u>p</u> <0.01)	0.38	0.42	0.50	0.51	0.68	0.64	0.50	0.55
Mean sim.	14.09	8.30	9.57	3.40	11.28	6.65	10.00	7.61
IASI obs.	7.96		7.54		10.23		7.72	

删除的内容: P

**Table 5 The NMBs and NMEs between the simulated and observed daily NH<sub>3</sub> VCDs by soil pH and month**

删除的内容: simulation

pH	Statistics (%)	January		April		July		October	
		E <sub>1</sub>	E <sub>2</sub>	E <sub>1</sub>	E <sub>2</sub>	E <sub>1</sub>	E <sub>2</sub>	E <sub>1</sub>	E <sub>2</sub>
pH>7.5	NMB	114.88	28.04	81.41	-38.99	43.3	4.24	67.99	46.95
	NME	117.8	49.27	89.23	44.38	56.11	48.13	71.49	57.44
7.5<=pH<6.5	NMB	92.82	9.19	44.6	-54.14	39.27	-10.78	44.01	11.13
	NME	95.83	34.16	64.13	54.7	52.52	45.54	52.54	37.69
pH<=6.5	NMB	41.61	-11.76	1.30	-67.41	-12.43	-55.81	8.64	-25.48
	NME	54.72	36.76	60.16	68.5	34.78	56.72	35.27	43.68

**Table 6 The modeling performance at JSPAES and SHPD in cases with different SO<sub>2</sub> and NO<sub>x</sub> emission estimates. The NMBs and NMEs were based on the observed and simulated hourly concentrations.**

Cases	JSPAES			SHPD			
	Increased/ Decreased %	NMB %	NME %	Increased/ Decreased %	NMB %	NME %	
NH <sub>3</sub>	Base case		1.73	56.94		32.32	98.36
	Case 1	10.14	11.09	59.02	11.67	47.54	102.68
	Case 2	-1.17	-0.59	57.85	-0.83	29.51	96.93
	Case 3	8.48	9.29	59.64	11.12	44.92	100.94
NH <sub>4</sub> <sup>+</sup>	Base case		15.01	42.27		84.45	100.23
	Case 1	-8.67	5.19	39.24	-10.99	62.53	84.93
	Case 2	1.87	17.55	45.40	1.40	87.40	102.37
	Case 3	-6.95	7.33	41.85	-10.36	65.69	86.27
SO <sub>4</sub> <sup>2-</sup>	Base case		14.38	43.65		91.92	110.18
	Case 1	-17.63	-4.90	40.81	-19.59	54.30	82.62
	Case 2	2.76	18.42	43.7	1.55	94.34	112.30
	Case 3	-14.91	-1.98	39.39	-18.45	55.96	83.67
NO <sub>3</sub> <sup>-</sup>	Base case		-6.55	44.81		29.46	93.69
	Case 1	1.25	-5.92	44.52	6.30	37.56	92.51
	Case 2	0.86	-5.85	46.71	-0.43	34.61	98.52
	Case 3	1.85	-4.90	46.51	5.78	42.85	97.19

Figure 1

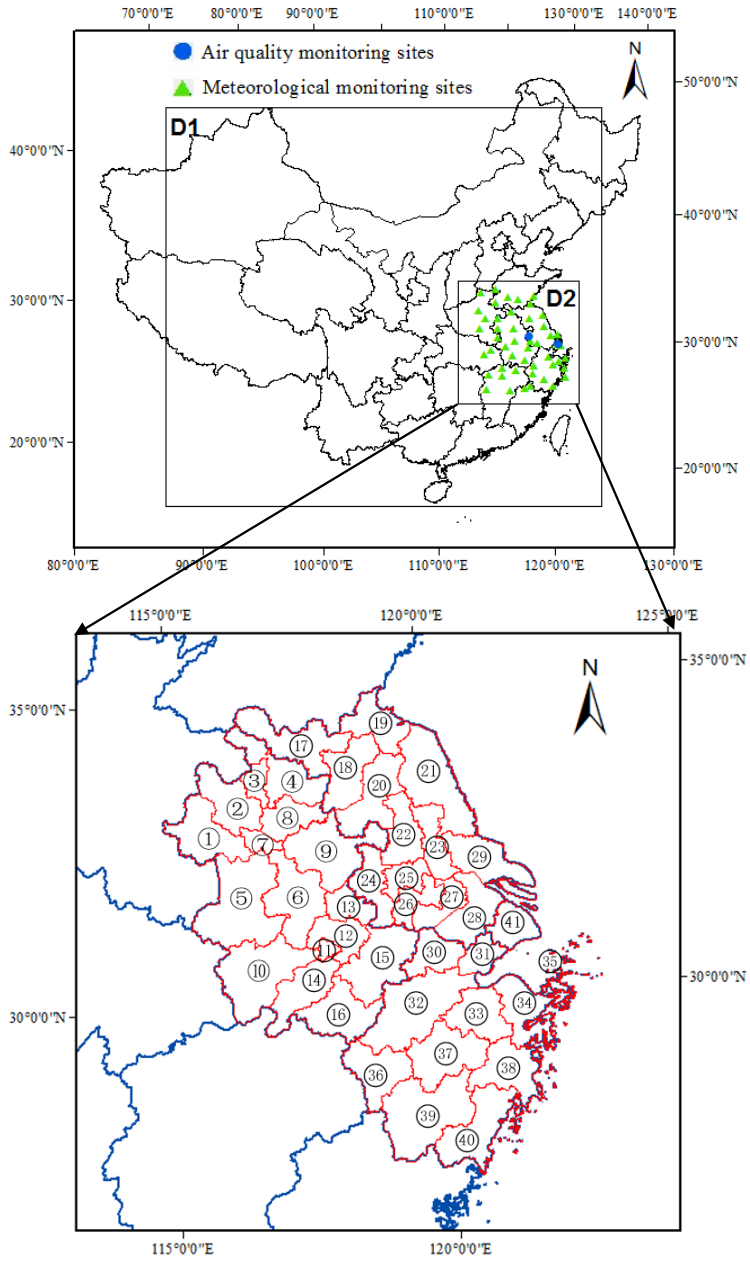


Figure 2

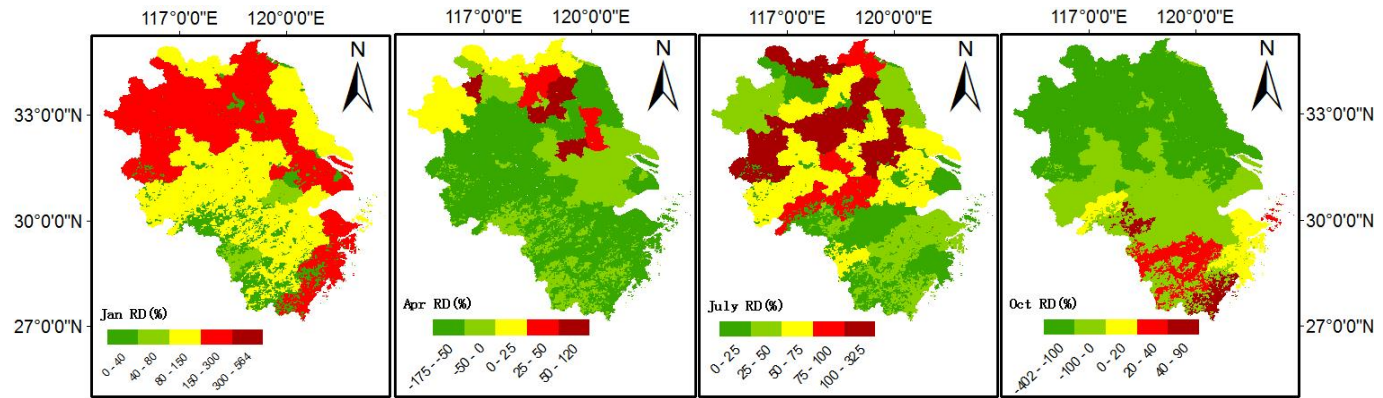
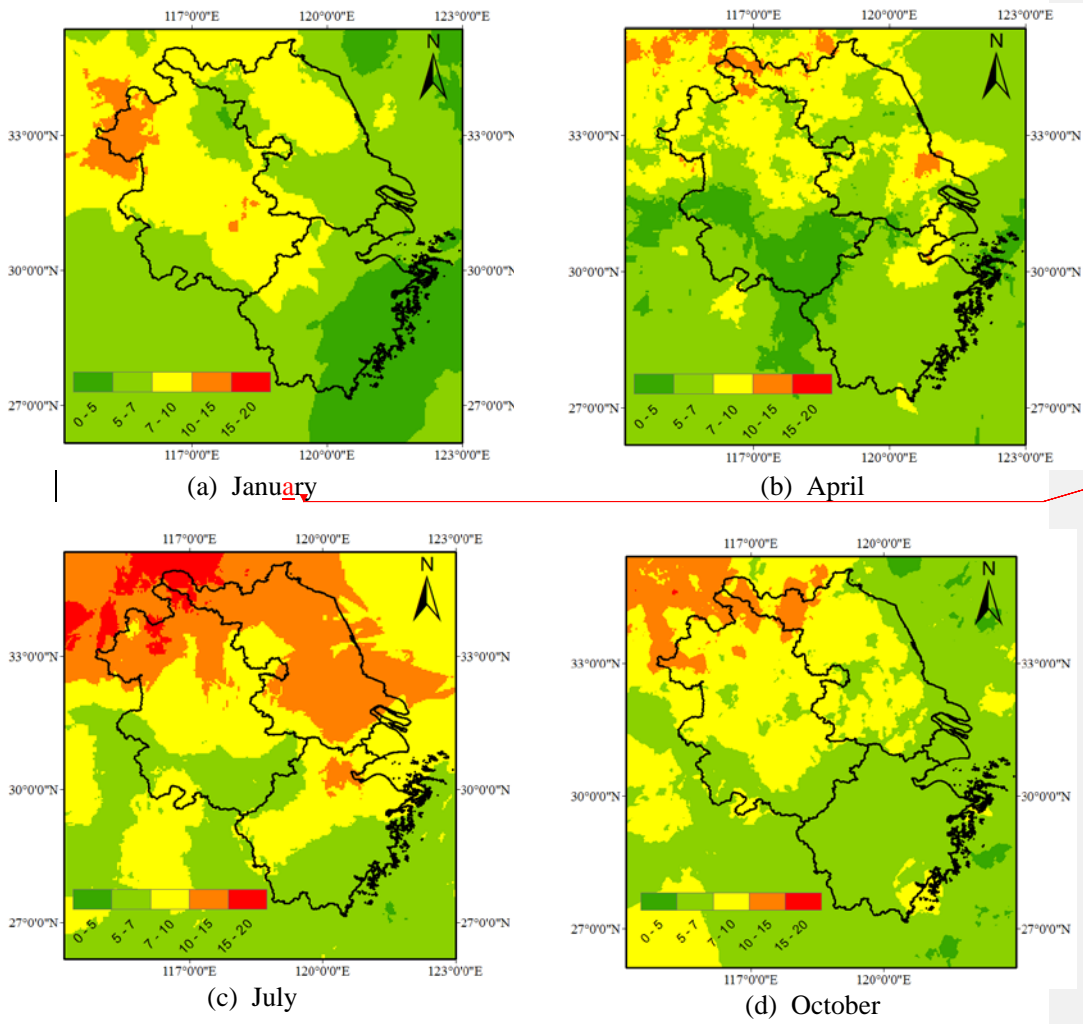




Figure 3



删除的内容: a

Figure 4

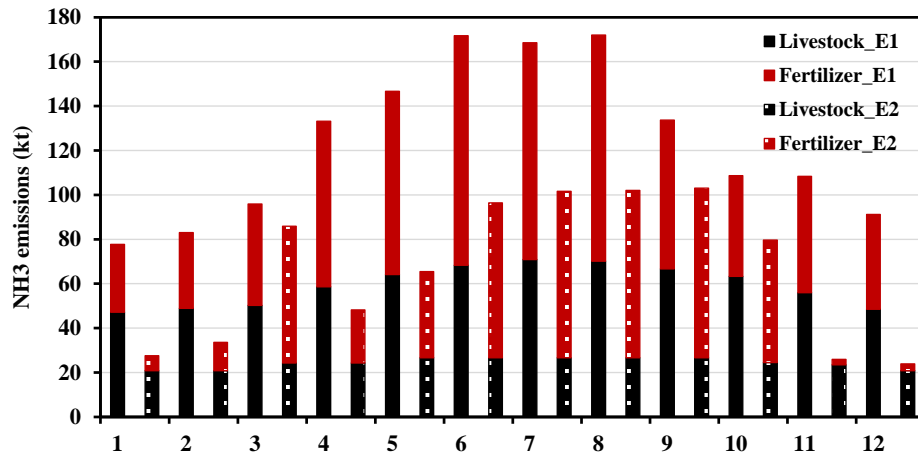
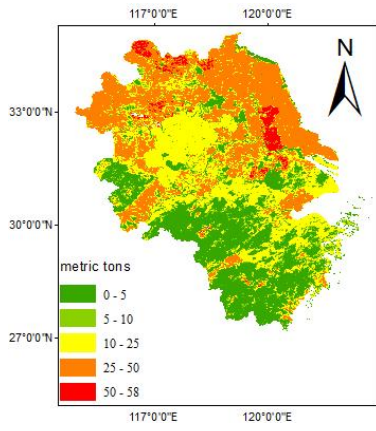
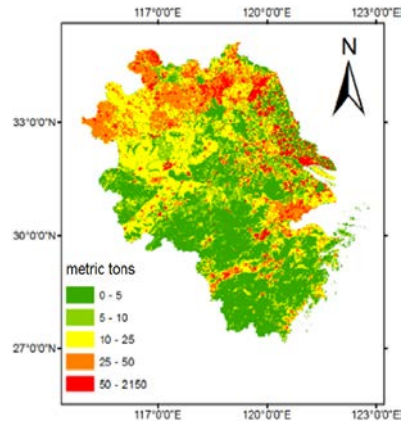


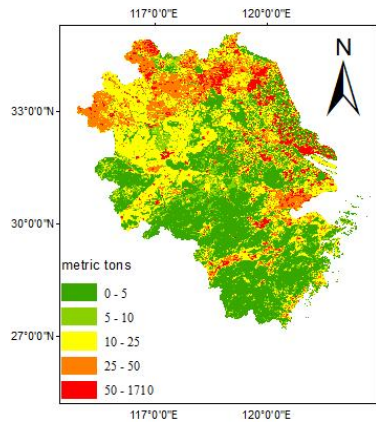
Figure 5



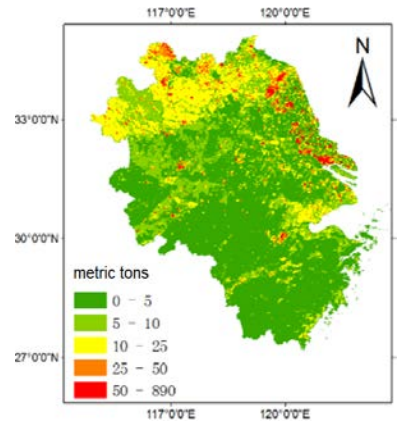
(a) Fertilizer use in E1



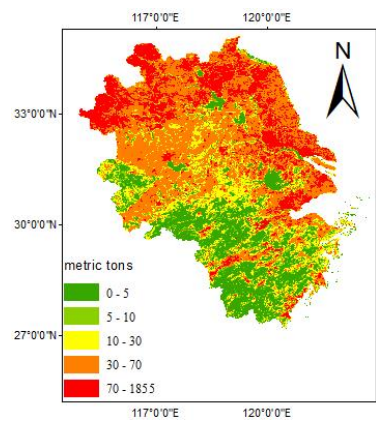
(b) Fertilizer use in E2



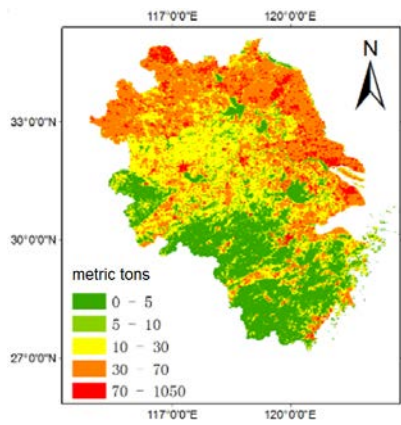
(c) Livestock farming in E1



(d) Livestock farming in E2

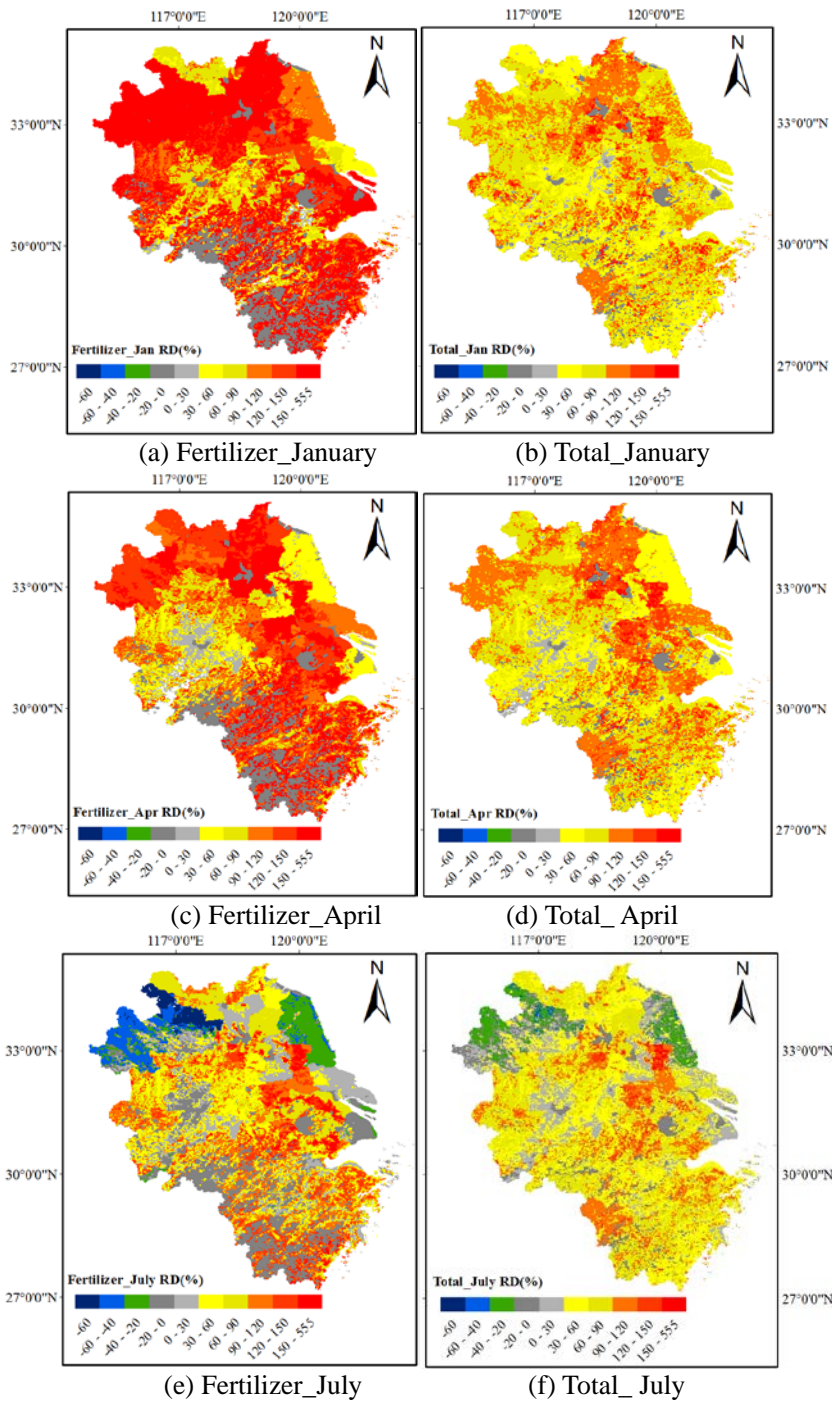


(e) Total emissions in E1



(f) Total emissions in E2

Figure 6



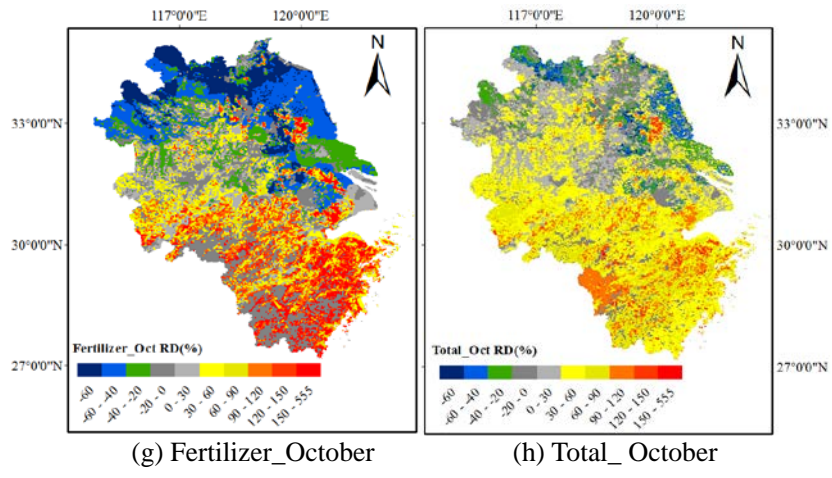


**Figure 7**

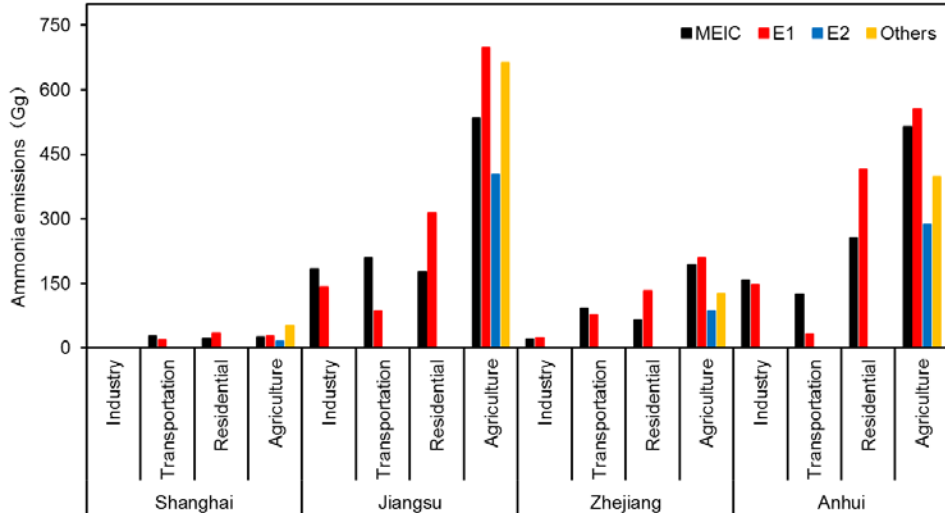
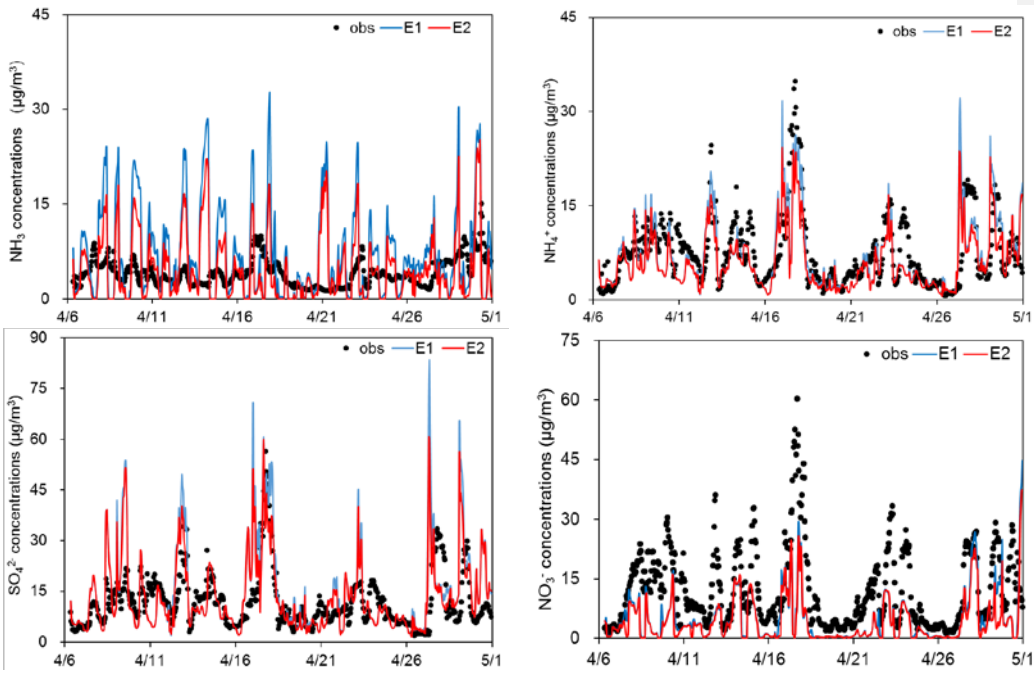
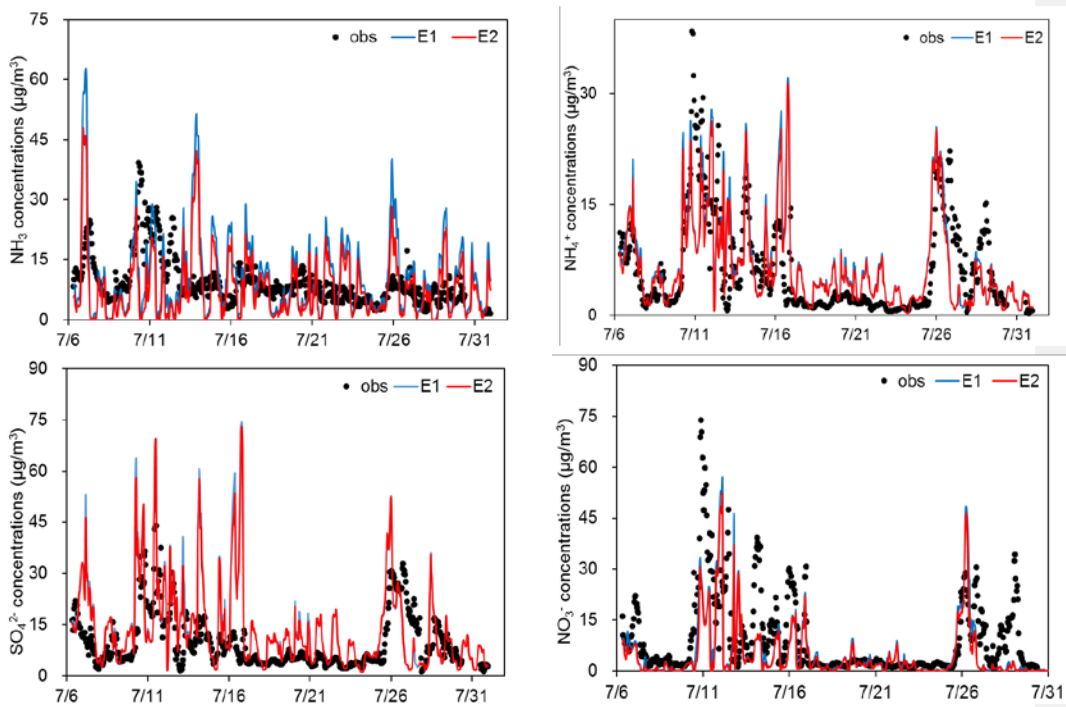


Figure 8

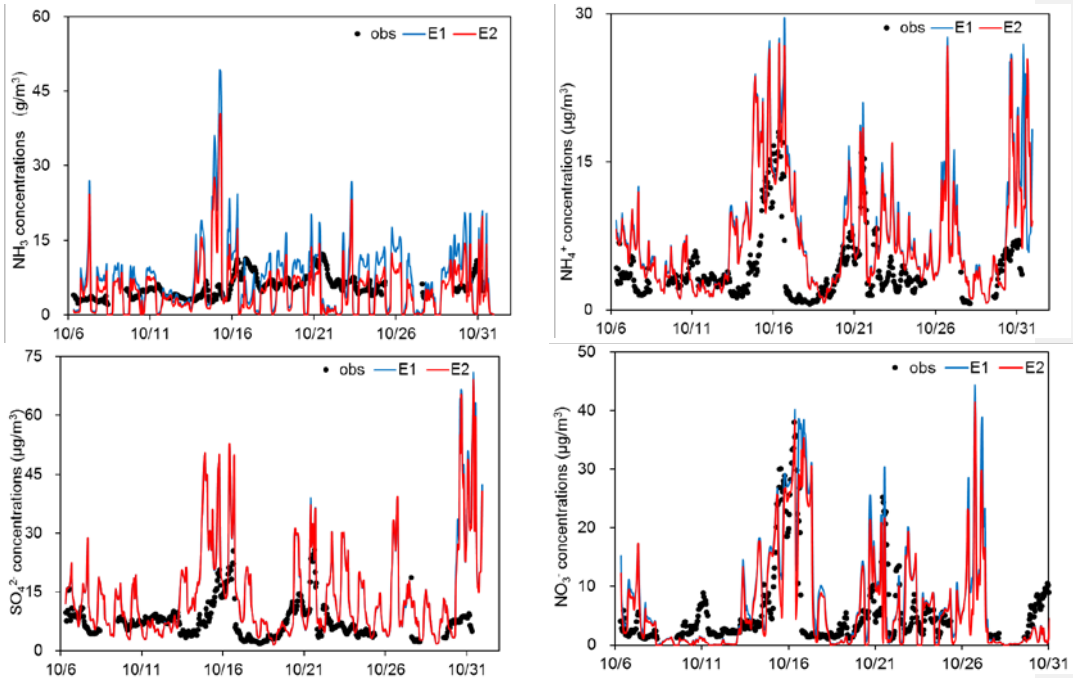


(a) SHPD\_April

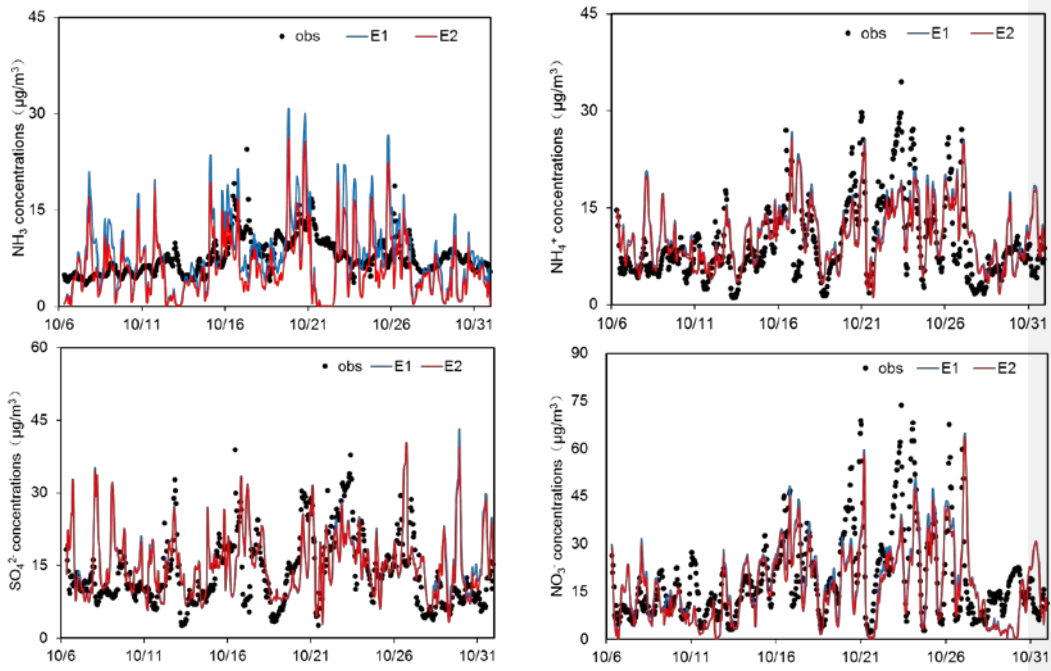


(b) SHPD\_July





(c) SHPD\_October



(d) JSPAES\_October



**Figure 9**

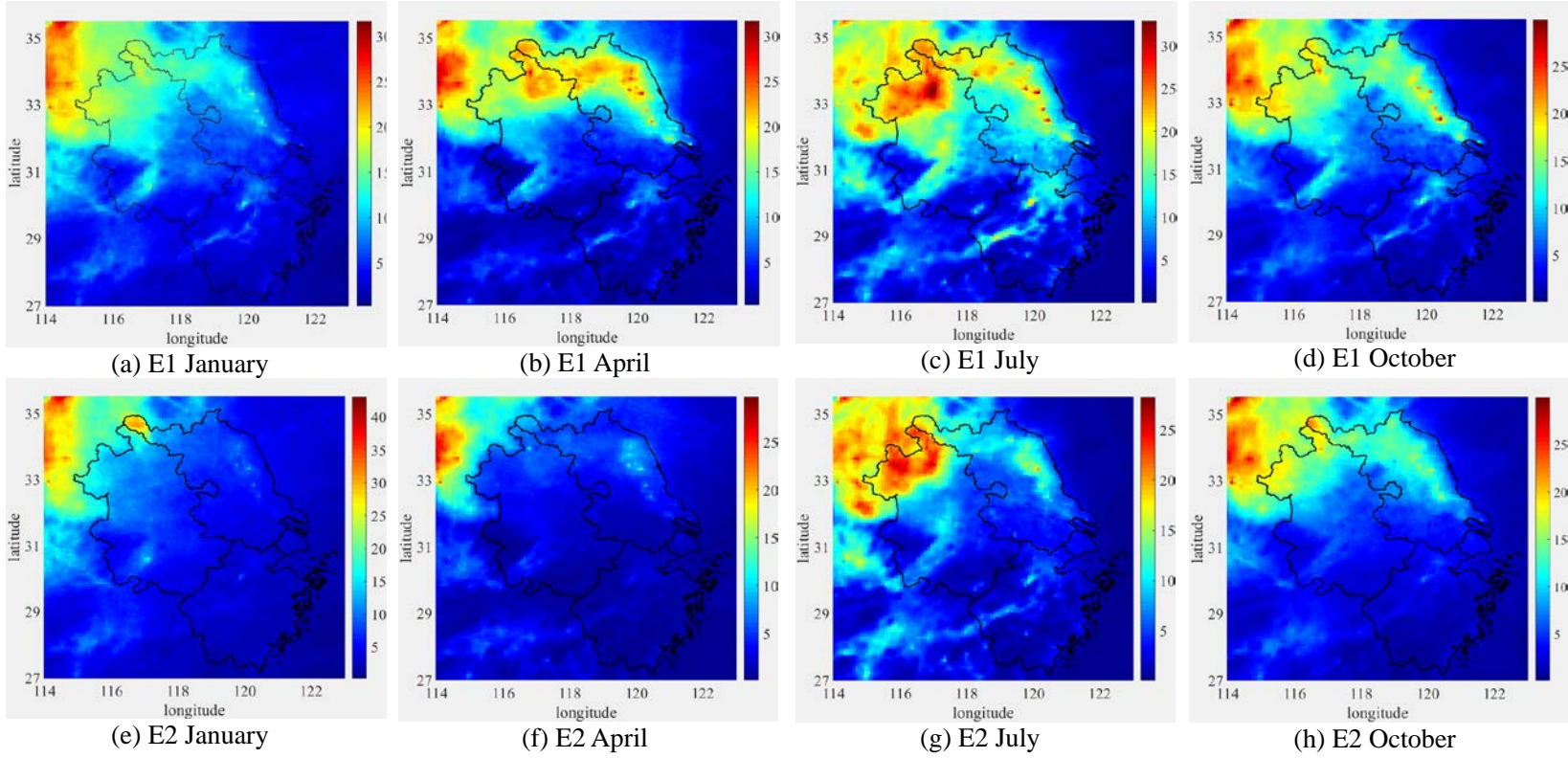


Figure 10

